

**NASA TECHNICAL  
TRANSLATION**



**NASA TT F-670**

*2.1*

**NASA TT F-670**

**LOAN COPY: RETURN  
AFWL (DOGL)  
KIRTLAND AFB, NM**

0069191



TECH LIBRARY KAFB, NM

# **PROBLEM SOLUTION BY THE "LARGE-PARTICLE" METHOD**

*by K. A. Vedyashkina, Z. F. Levina, S. P. Lomnev,  
G. P. Prudkovskiy, T. V. Rastopchina, G. V. Ruben,  
and V. V. Yurchenko*

*Transactions of the Computer Center  
Academy of Sciences, USSR  
Moscow, 1970*

**NATIONAL AERONAUTICS AND SPACE ADMINISTRATION • WASHINGTON, D. C. • JULY 1971**



PROBLEM SOLUTION BY THE  
"LARGE-PARTICLE" METHOD

By K. A. Vedyashkina, Z. F. Levina, S. P. Lomnev,  
G. P. Prudkovskiy, T. V. Rastopchina,  
G. V. Ruben, and V. V. Yurchenko

Translation of "Resheniye Zadach Metodom Krupnykh Chastits"  
Transactions of the Computer Center, Academy of Sciences, USSR  
Moscow, 1970

NATIONAL AERONAUTICS AND SPACE ADMINISTRATION

---

For sale by the National Technical Information Service, Springfield, Virginia 22151  
\$3.00



PROBLEM SOLUTION BY THE  
"LARGE-PARTICLE" METHOD

Editor-in-chief: S. P. Lomnev,  
Doctor of Physics and  
Mathematical Sciences

TABLE OF CONTENTS

Introduction . . . . .	1
The Movement of Charged Particles in an Electric Field . . . . .	3
Two-dimensional Problem of the Behavior of a Cloud of Charged Particles in a Magnetron . . . . .	6
Investigation of the Particle-in-Cell Method . . . . .	17
Some Questions in the Calculation of the Evolution of Stars . . . . .	51

## INTRODUCTION

/3\*

Methods, based on replacing the continuity equations or their analogs by "large-particle" equations of motion, are now finding application in the solution of problems in electrodynamics, gas dynamics, hydrodynamics and even solid-state physics. This method has given good results in a number of problems where classical methods encounter difficulties.

Two steps can be identified:

- 1) the "particle" motion during  $\Delta t_i$  is calculated in a given field;
- 2) from the new "particle" configuration the fields are calculated for a new determination of the motion during  $\Delta t_{i+1}$ .

The "large particle" itself has various geometrical shapes: point, ring, disk, rod, filament.

The details of the problems and the necessity of adapting different variations of the method to them give birth to an abundance of procedures and a confusion in terminology is possible. It seems appropriate to us to identify three basic methods in terms of the nature of the interaction to be calculated:

1. The straightforward "large-particle" method. The fields are known functions of the coordinates and velocities. The problem is solved in one step: only the particle motion is calculated. Because of its simplicity this method has been used to solve several electrodynamic problems.

2. The "average density" method. A region is marked off into a three-dimensional lattice; the density is calculated for an arrangement of a finite number of test particles, whose motion in the time interval  $\Delta t_{i+1}$  is found from the dynamic equations with the forces determined by this density at a previous instant of time  $t_i$ .

3. In the Harlow "particles in cells", or PIC, method the solution is carried out in three steps:

- a) preliminary values of the fields are found during the time interval  $\Delta t_i$  in an Eulerian network of cells, fixed with respect to the observer;
- b) the motion of the masses is determined from the equations of motion in a Lagrangian network of particles;
- c) the field corrections, associated with particle motion, are calculated.

/4

---

\*Numbers in the margin indicate pagination in the foreign text.

The PIC method has been found to be quite consistent in a number of gas-dynamics problems.

This collection of papers contains examples of problems solved by these three methods. They do not represent a detailed physical investigation, but, instead, they illustrate the calculational possibilities.

# THE MOVEMENT OF CHARGED PARTICLES IN AN ELECTRIC FIELD

/5

K. A. Vedyashkina, T. V. Rastopchina

ABSTRACT: Application of the PIC method to calculation of motion of charged particles in an electric field is examined.

In some problems it is advantageous to use the straightforward "large-particle" method. The volume  $V_0$  containing charges at  $t = 0$  is divided into small volume elements  $\Delta V_m$  (the volume elements can be equal in size), and each charge, contained in  $\Delta V_m$  is concentrated at its center. It is considered as a new "enlarged particle". Altogether,  $M$  "particles" are obtained, whose motion is determined by the systems of motion equations:

$$\left. \begin{aligned} \frac{d\vec{P}_m}{dt} &= e_m \left\{ \vec{E}_m + \frac{[\vec{R}_m \vec{H}_m]}{c} \right\}; \\ \vec{E}_m &= \vec{E}_{0m} + \vec{E}_{1m}; \\ \vec{H}_m &= \vec{H}_{0m} + \vec{H}_{1m}, \quad m = 1, 2, \dots, M. \end{aligned} \right\} \quad (1)$$

$\vec{E}_{0m}$ ,  $\vec{H}_{0m}$  are the external electric and magnetic fields at the  $R_m$ -th point;  $\vec{E}_{1m}$ ,  $\vec{H}_{1m}$  are terms that take account of the interaction of the  $m$ -th "particle" with all the others.

Averages over the particles within  $\Delta V_m$  ( $m = 1, 2, \dots, M$ ) are taken as the initial conditions. In this it is assumed that during the time  $0 < t < T$  the active particles in the volumes  $\Delta V_m$  act as a unit; this is a permissible assumption for finite  $T$  (the particle transit time) and for sufficiently small  $\Delta V_m$  when long-range interactions predominate over short-range within  $\Delta V_m$ . The permissible size of  $\Delta V_m$  depends on the coefficients and on the spread of the initial velocities in  $\Delta V_m$ . It is determined by the convergence of the solutions of Eqs. (1) for an additional decrease in  $\Delta V_m$  [1].

/6

The effect of near collisions of the  $i$ -th and  $j$ -th particles is excluded by the introduction of a "protective cube", the dimensions of which are determined on the basis of an experimental analysis or the following simple considerations. Let the scattering of a particle with charge  $e_j$  by particles with charge  $e_i$  be expressed by the well-known Rutherford formula and the scattering force is

$$\bar{F} = \lambda \frac{2\pi}{m_i} e_j^2 e_i^2 n_i \frac{\bar{u}}{u^3},$$

where  $\bar{u}$  is the relative velocity;  $\lambda$  is the "Coulomb logarithm",

$$\lambda = \int_0^{r_{\max}} \frac{r dr}{r_1^2 + r^2}; \quad r_1 = \frac{e_i e_j}{m_i u^2}.$$

Dividing  $\lambda$  into  $\lambda_b = \int_0^{2r_1} \frac{r dr}{r_1^2 + r^2}$  and  $\lambda_g = \int_{2r_1}^{r_{\max}} \frac{r dr}{r_1^2 + r^2}$  for  $r_1 \ll r_{\max}$ , we obtain

a "protective cube" size of the order of  $r_1$  [2].

As an example let us consider a constant-current electron beam, moving in space with a uniform electric field  $E_{z0} = \text{const}$ ,  $E_{x0} = 0$ ,  $E_{y0} = 0$  for  $z_0 < z < L$ . It is simulated by "large particles", emerging from the slit in time  $\Delta t$ , whose charge is  $q_k = I(t_k) \Delta t$ ,  $v_{k0}(t_k) = v_0$ ,  $t_k = t_0 + (k-1) \Delta t$ ,  $z_{k0}(t_k) = z_0$ .

Let us assume that at the  $t_k$  instant of time one "particle" emerges. When  $z_m > L$ , the "particle" no longer needs to be considered. Then the equation of motion will be

$$z_m = A_0(E + E_{z1m}); \quad E_{z1m} = \sum_{i \neq m} \frac{e_i z_{mi}}{|z_{mi}|^3}, \quad (2)$$

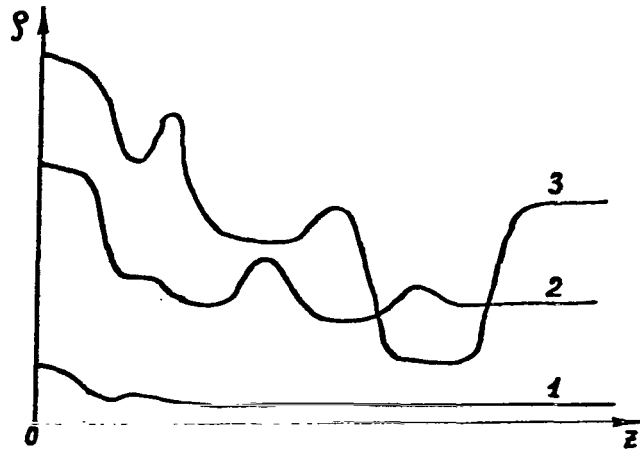
$$m = 1, 2, \dots, k; \quad k = 1, 2, \dots, K,$$

where  $A_0 = \frac{e}{c^2 m_0}$ ;  $e$  is the electron charge and  $m$  is the electron mass;  $c$  is the velocity

of light;  $0 \leq z(t) \leq L$ ;  $0L$  is the field-filled gap; differentiation is with respect to  $ct$ .

In the process of solving (2) the particles are accumulated in the interval  $0L$ ;  $\Delta t$  is selected from trial calculations. Each particle is surrounded by an  $\varepsilon$ -region to exclude collisions.





Graph of  $\rho(z)$ :

1 - for  $I = I_0$ , 2 - for  $I = 6I_0$ , 3 - for  $I = 9I_0$ .

To calculate the charge density  $\rho$  with 1% accuracy it was found adequate that  $M = 300$ ,  $\Delta ct = 3$ ;  $v_0$  was taken equal to  $0.01c$  and  $L = 10$  cm. The figure shows the distribution  $\rho(z)$  at some instant of time. It is not hard to see that as the current increases,  $\rho(z)$  becomes more and more nonuniform and fluctuations appear, caused by Coulombic interaction.

#### REFERENCES

1. Lomnev, S. P. The Effect of Coulomb Repulsion on Particle Bunching in a Linear Electron Accelerator. Dokl. Akad. Nauk SSSR, 135, No. 4, 1960.
2. Lomnev, S. P. Raschet i issledovaniye elektrofizicheskikh ustanovok i elektrofizicheskikh yavleniy na tsifrovyykh vychislitel'nykh mashinakh (The Analysis and Study of Electrophysical Apparatus and Electrophysical Phenomena on Digital Computers). VTs (Computer Center) Akad. Nauk SSSR, Moscow, 1965.

# TWO-DIMENSIONAL PROBLEM OF THE BEHAVIOR OF A CLOUD OF CHARGED PARTICLES IN A MAGNETRON

/8

K. A. Vedyashkina, G. P. Prudkovskiy

ABSTRACT: Application of the PIC method to behavior of electron beams is discussed.

Magnetron design by computer is now possible (see [1]). This paper considers the self-consistent motion of a large number (of the order of a thousand) of charged particles, representing electron beams.

In this paper the analysis is applied to the magnetron type of continuous-operation oscillator [2, 3].

The interaction region is a rectangle which is subdivided by a constant-interval gridwork for calculating the space-charge field by the "average-density" method [4].

The charge density  $\rho(x, y, t)$  is calculated from the disposition of test particles at the end of a time interval  $\Delta t$  and determines the field acting on the particles during the subsequent interval.

The equations of motion can be written in the following form:

$$\left. \begin{aligned} \ddot{x} &= A_0 (E_x + \dot{y} H_z); \\ \ddot{y} &= A_0 (E_y - \dot{x} H_z); \\ A_0 &= \frac{e}{m_0 c^2}, \end{aligned} \right\} \quad (1)$$

the time is in length units ( $ct$  instead of  $t$ ).

Let us examine  $E = E_0 + E_\lambda + E_\rho$ . We assume the d-c field is uniform  $E_0 = E_{0y} = -\frac{u_a}{d}$ , where  $u_a$  is the anode potential and  $d$  is the width of the active space.

Such an approximation is permissible for a one-row magnetron in which the cathode is continuous, as in the normal magnetrons.

In the high-frequency field let us isolate one spatial harmonic (see [2])

9

$$\left. \begin{aligned} E_{\lambda, x} &= E_1 \operatorname{sh} g y \cos g(x - v_{ph} t); \\ E_{\lambda, y} &= E_1 \operatorname{ch} g y \sin g(x - v_{ph} t), \end{aligned} \right\} \quad (2)$$

where  $g = \frac{2\pi}{l}$ ,  $v_{ph} = c/\lambda$ ,  $l = 1$  cm is the period of the system.

The space-charge field  $E_\rho$  is determined by the potential, for which

$$\Delta \Phi(x, y, t) = -4\pi \rho(x, y, t), \quad (3)$$

with  $\Phi = 0$  for  $y = 0$  and  $y = d$ ,

$$\Phi_\rho(x, y, t) = \Phi_\rho(x + l, y, t). \quad (4)$$

The magnetic field is uniform ( $H_z = H$ ).

The portion of the cathode emitting into the nigonron is small:  $\delta \times b$  ( $b$  is the system dimension along the  $z$ -axis). In each time interval  $k$  particles, equidistant from the  $x$ -axis over the segment  $\delta$  ( $\delta = 0.2l$ ,  $b = 10l$ ), are emitted simultaneously.

Let us examine possible ways of solving the equations of motion. The method recommended in [1] uses a special form of Eqs. (1). The Eqs. (1) are written in complex form

$$\ddot{z} + i w_c \dot{z} = A_0 E, \quad (5)$$

where  $w_c = A_0 H$ ;  $z = x + iy$ ;  $E = E_x + iE_y$ ;

we find

$$z = z_0 - \frac{\dot{z}_0}{i w_c} \left\{ 1 - e^{-i w_c (t - t_0)} - A_0 \int_{t_0}^t E(\xi) \left[ 1 - e^{-i w_c (t - \xi)} \right] d\xi \right\}.$$

Assuming  $E(\xi) = E(t_p)$  ( $p$  is the interval number) in  $\Delta t$ , we obtain

$$\left. \begin{aligned} x_{p+1} &= x_p + \frac{\dot{y}_p}{w_c} (\cos w_c \Delta t - 1) + \frac{\dot{x}_p}{w_c} \sin w_c \Delta t + \\ &+ \frac{A_0}{w_c^2} \{ E_x^p (1 - \cos w_c \Delta t) - E_y^p (w_c \Delta t - \sin w_c \Delta t) \}; \end{aligned} \right\} \quad (6)$$

$$\left. \begin{aligned}
 y_{p+1} &= y_p - \frac{\dot{y}_p}{w_c} (\cos w_c \Delta t - 1) - \frac{y_p}{w_c} \sin w_c \Delta t + \\
 &+ \frac{A_0}{w_c^2} \{ E_y^p (1 - \cos w_c \Delta t) - E_x^p (w_c \Delta t - \sin w_c \Delta t) \}; \\
 x_{p+1} &= -\frac{w_c}{2} \left\{ (y_p - y_{p+1}) - \frac{(x_{p+1} - x_p)}{1 - \cos w_c \Delta t} \sin w_c \Delta t + \right. \\
 &+ \frac{A_0}{w_c^2} \left[ E_y^{p+1} \left( \frac{w_c \Delta t \sin w_c \Delta t}{1 - \cos w_c \Delta t} - 2 \right) - E_x^{p+1} w_c \Delta t \right] \Bigg\}; \\
 \dot{y}_{p+1} &= -\frac{w_c}{2} \left\{ x_{p+1} - x_p - \frac{(y_{p+1} - y_p) \sin w_c \Delta t}{1 - \cos w_c \Delta t} + \right. \\
 &+ \frac{A_0}{w_c^2} \left[ E_x^{p+1} \left( 2 - \frac{w_c \Delta t \sin w_c \Delta t}{1 - \cos w_c \Delta t} \right) - E_y^{p+1} w_c \Delta t \right] \Bigg\}.
 \end{aligned} \right\} \quad (6)$$

Besides the analysis in accordance with the scheme given, the equations were also solved by the Runge-Kutta method.

Let us compare the errors in one interval  $\Delta t$  of the analysis. According to the method of [1]

$$R = R_x + i R_y = -\frac{A_0}{6} \frac{dE}{dt} \Big|_{t_p + \theta_2 \Delta t} e^{-i\theta_1 w_c \Delta t} \Delta t^3, \quad 0 \leq \theta_1 \leq 1; 0 \leq \theta_2 \leq 1. \quad (7)$$

According to the Runge-Kutta method

$$\left. \begin{aligned}
 R_x + \Delta t^3 \left\{ \frac{A_0}{6} \frac{dE_x}{dt} \Big|_{t_p + \theta_1 \Delta t} - \frac{A_0}{6} \frac{dE_x}{dt} \Big|_{t_p + \theta_2 \Delta t} - \frac{A_0^2 H}{4} (E_y - iH) \Big|_{t_p + \theta_1 \Delta t} - \right. \\
 \left. - \frac{A_0 H}{6} (E_y - iH) \Big|_{t_p + \theta_2 \Delta t} - \frac{A_0}{4} (E_x - iH) \Big|_{t_p + \theta_1 \Delta t} \right\}; \\
 \left. \begin{aligned}
 t &= t_p + \Delta t; \\
 x &= x(t_p) + x(t_p) \Delta t + \frac{\theta_2 \Delta t^2}{2} x(t_p + \theta_2 \Delta t); \\
 y &= y(t_p) + y(t_p) \Delta t + \frac{\theta_2 \Delta t^2}{2} y(t_p + \theta_2 \Delta t)
 \end{aligned} \right\}; \\
 R_y + \Delta t^3 \left\{ \frac{A_0}{6} \frac{dE_y}{dt} \Big|_{t_p + \theta_1 \Delta t} - \frac{A_0^2 H}{6} (E_x - iH) \Big|_{t_p + \theta_1 \Delta t} - \frac{A_0}{6} \frac{dE_y}{dt} \Big|_{t_p + \theta_2 \Delta t} + \right. \\
 \left. + \frac{A_0^2 H}{4} (E_x - iH) \Big|_{t_p + \theta_2 \Delta t} - \frac{A_0}{4} (E_x - iH) \Big|_{t_p + \theta_2 \Delta t} \right\} \quad \begin{aligned} &0 \leq \theta_i \leq 1, \\ &i = 1, 2, 3, 4. \end{aligned}
 \end{aligned} \right\} \quad (8)$$

Thus, both errors are of the order of  $\Delta t^3$ . Sample calculations showed that both procedures require the same amount of time to calculate trajectories with the same interval. The interval, required for the calculation, was selected from a comparison of the results; it must not be greater than  $T_\lambda/50$ . For the calculations it is recommended that an interval be taken such that a particle passed through, on the average, one cell of the point lattice. /11

The calculation of the space-charge field is based on solving Poisson's equation in finite differences. For the  $i, j$  lattice element we have

$$\frac{\Phi_{i+1,j} - 2\Phi_{i,j} + \Phi_{i-1,j}}{\tau^2} + \frac{\Phi_{i,j+1} - 2\Phi_{i,j} + \Phi_{i,j-1}}{h^2} = -4\pi\epsilon_{ij}, \quad (9)$$

where  $\tau = \frac{d}{N}$ ;  $h = \frac{l}{M}$ ;  $\rho_{i,j} = \frac{m_{ij}q}{4\pi\tau b}$ ;  $M$  is the number of elements along the  $x$ -axis;  $N$  is the number of elements along the  $y$ -axis;  $m_{i,j}$  is the number of particles in four rectangles surrounding the point  $(i, j)$ . The charge of the test particle is chosen from the condition

$$I_e \Delta t = qk. \quad (10)$$

The boundary conditions are

$$\Phi_{0,j} = 0; \quad \Phi_{N,j} = 0; \quad \Phi_{i,0} = \Phi_{i,M}. \quad (11)$$

The field is determined by solving a set of  $N \times M$  linear equations. In [1] the potential is represented in Fourier series. In our work we used the Seidel iteration method, which is suitable for this problem because the values  $\Phi_{i,j}$ , obtained in the previous interval and differing from the desired values, are taken as the zero approximation. Therefore the iteration process converges quickly. The field components can be found from the formulas

$$\left. \begin{aligned} E_x &= \frac{\Phi_{i,j+1} - \Phi_{i,j}}{h}(\tau - \tau') + \frac{\Phi_{i+1,j+1} - \Phi_{i+1,j}}{h} \tau'; \\ E_y &= \frac{\Phi_{i+1,j} - \Phi_{i,j}}{\tau}(h - h') + \frac{\Phi_{i+1,j+1} - \Phi_{i,j+1}}{\tau} h. \end{aligned} \right\} \quad (12)$$

The calculations were performed on a BESM-6 computer. To ascertain the parameters required for the analysis the trajectories were calculated for different numbers of particles and different numbers of lattice elements. It is found that a  $15 \times 30$  lattice is adequate for a current  $I_e = I_a$  and  $u_a = 20$  kV; at least 6 particles must be emitted during the interval  $\Delta t = T_\lambda/60$ . For a higher current, as seen from Fig. 1, there is an

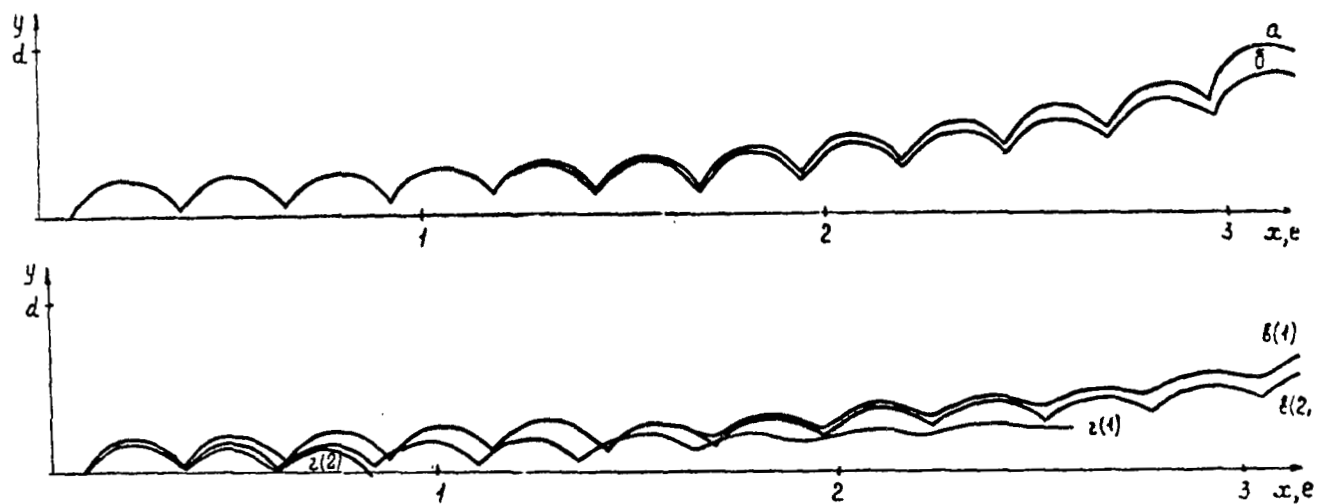


Figure 1. Particle Trajectories for Different  $I_e$ :

a -  $I_e = 0$  (ignoring space charge); b -  $I_e = 1$  A; c -  $I_e = 3$  A: 1)  $15 \times 30$  lattice; 2)  $30 \times 60$  lattice;  
 d -  $I_e = 5$  A: 1)  $15 \times 30$  lattice; 2)  $30 \times 60$  lattice.

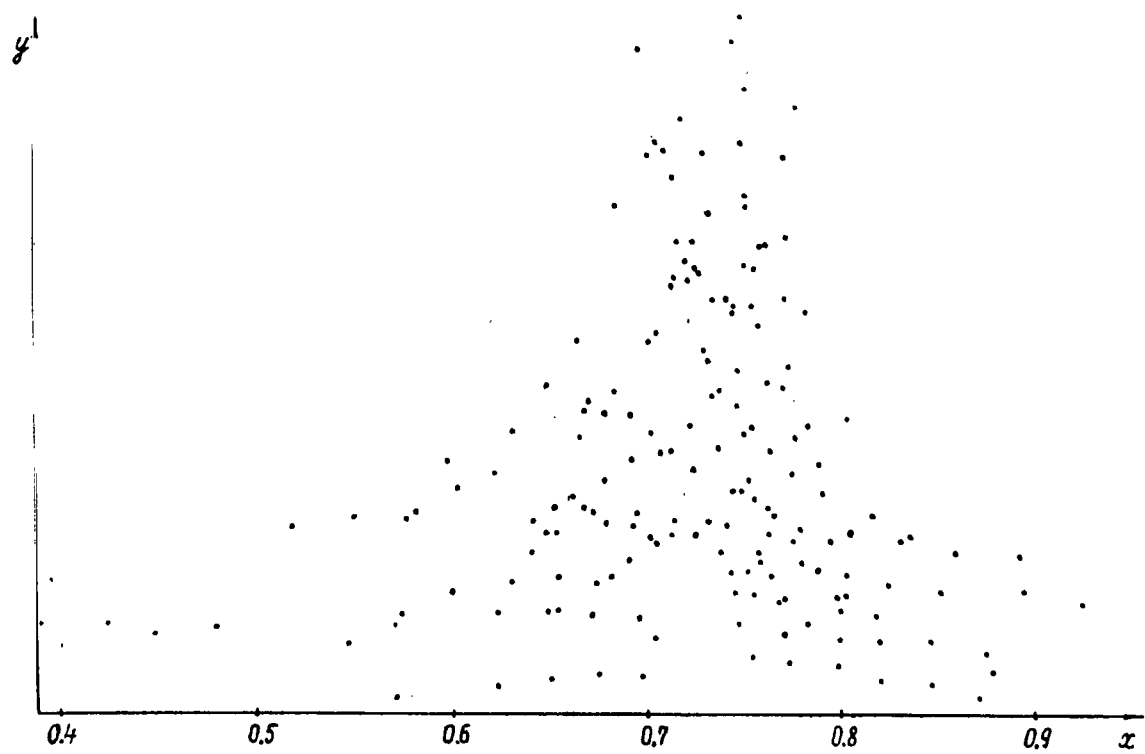


Figure 2. General Shape of the Electron Cloud in a Planar Magnetron,  $I_e = I_0$ .

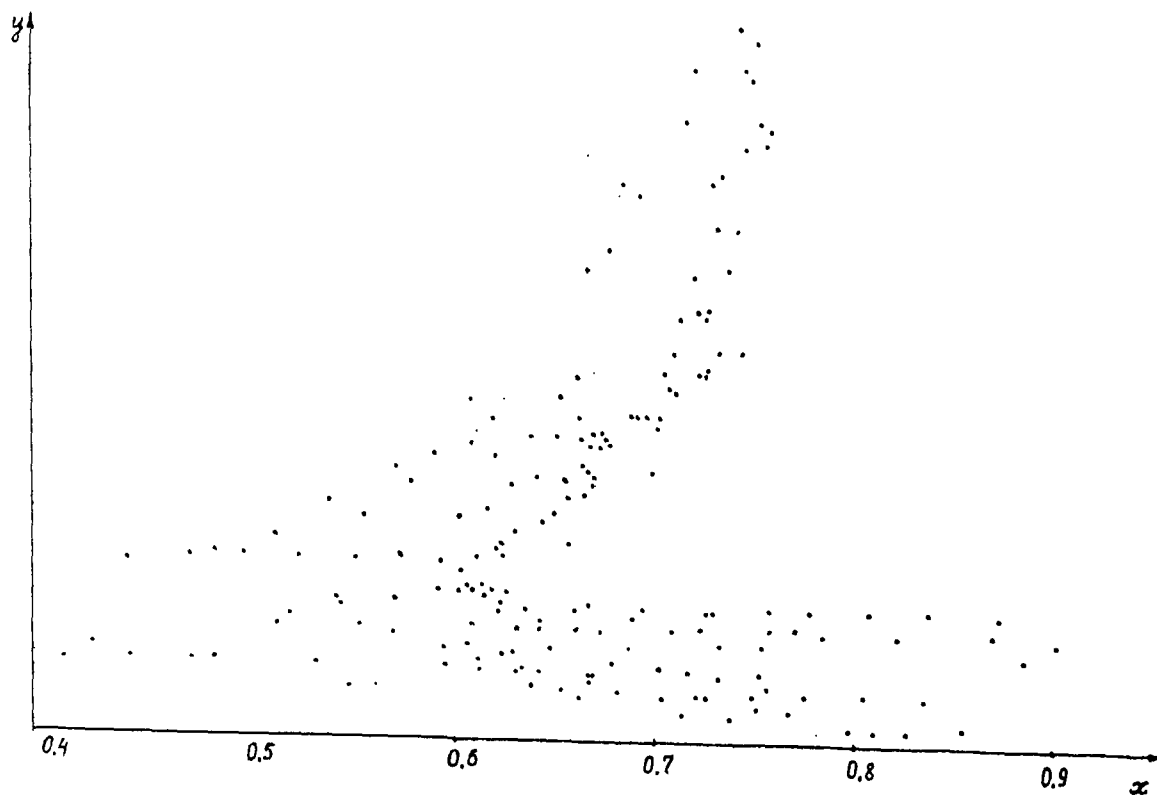


Figure 3. General Shape of the Electron Cloud in a Planar Magnetron,  $I_e = 4I_0$ .



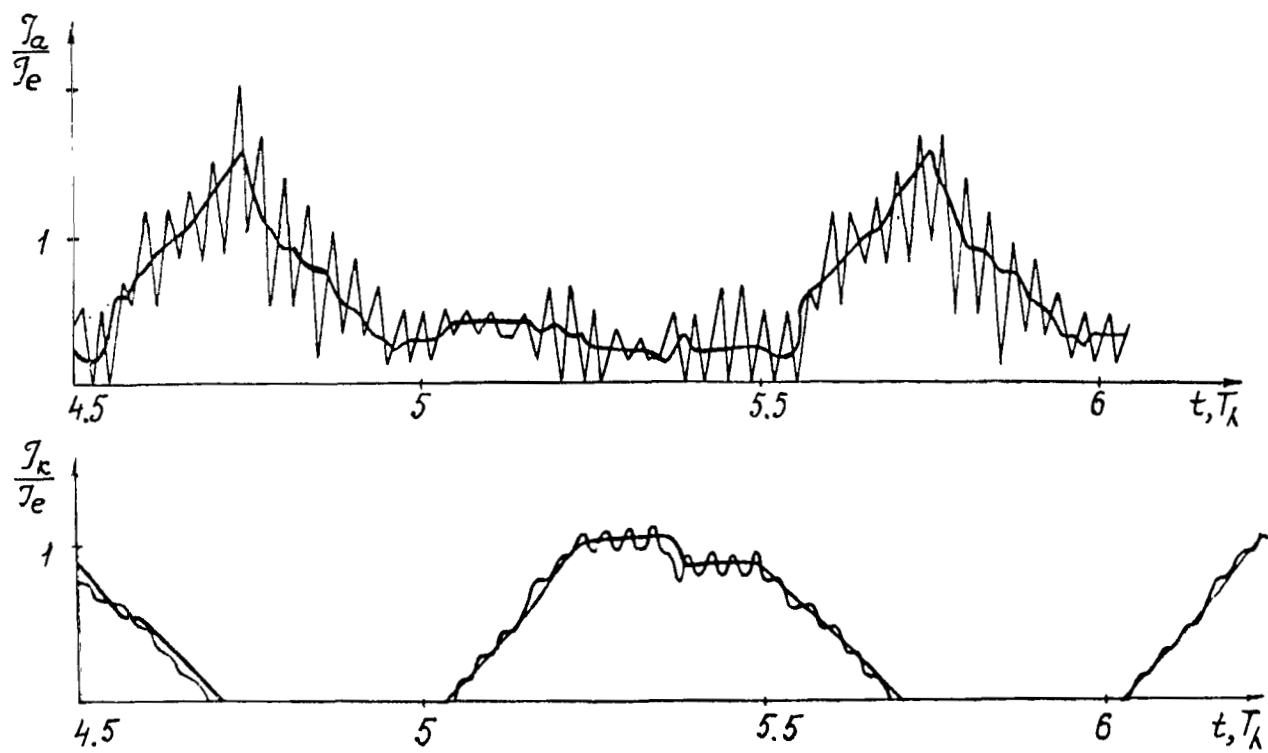


Figure 4. The Dependence of  $I_a/I_e$  and  $I_k/I_e$  on  $t$  for  $I_e = 0$  for  $k = 6$ ,  $k = 12$ .

appreciable difference between the trajectories plotted for  $15 \times 30$  and  $30 \times 60$  lattices. At 5 amperes the character of the trajectory is altered qualitatively when one goes over to the more precise solution.

It should be noted that the effect of the space charge is a slowing of the drift of particles to the anode. Characteristically its effect is to reduce the amplitude of the cyclotron oscillations. In Fig. 2 the particle coordinates are shown for a fixed instant of time. They form the typical magnetron tongue. Figure 3 shows the tongue for a current that is four times higher than in Fig. 2. The tongue "blowing-away" effect, described in [2], is clearly seen. Figures 4, 5 and 6 illustrate the change in anode and cathode current for different analysis parameters and for different emission currents. Figure 4 shows current graphs ignoring the space charge for 6 and 12 particles emitted during  $\Delta t$ . An increase in the number of particles causes a flattening of the graphs. It is significant, however, that a simple averaging of the oscillations gives the same effect.

In Figs. 5 and 6 the currents are 3 A and 5 A, respectively; graphs are given for different analysis parameters. As the analysis is refined, a splitting of the cathode-current maximum is observed. The calculation time amounts to 45 minutes (30 minutes when interaction is ignored) for  $10 T_\lambda$  periods (600 time intervals) for an emission of 12 particles/ $\Delta t$  and a  $30 \times 60$  lattice.

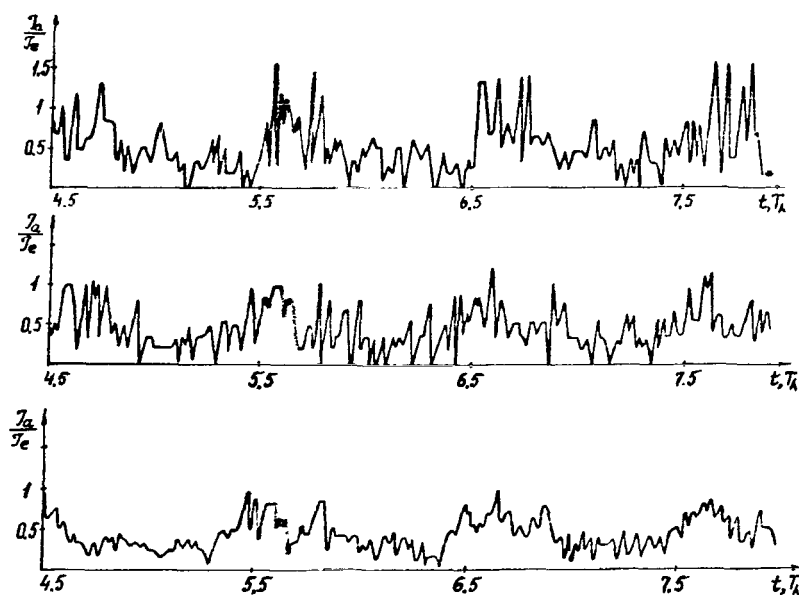


Figure 5. The Dependence of  $I_a/I_e$  on  $t$  for  $I_e = 3$  A for  $k = 6$ ,  $15 \times 30$  lattice;  $k = 6$ ,  $30 \times 60$  lattice;  $k = 12$ ,  $30 \times 60$  lattice.

This paper is methodological in nature. The calculations in accordance with the program formulated indicated the possibility of studying the physical processes, occurring in a magnetron-type oscillator, with the aid of a BESM-6 type computer.

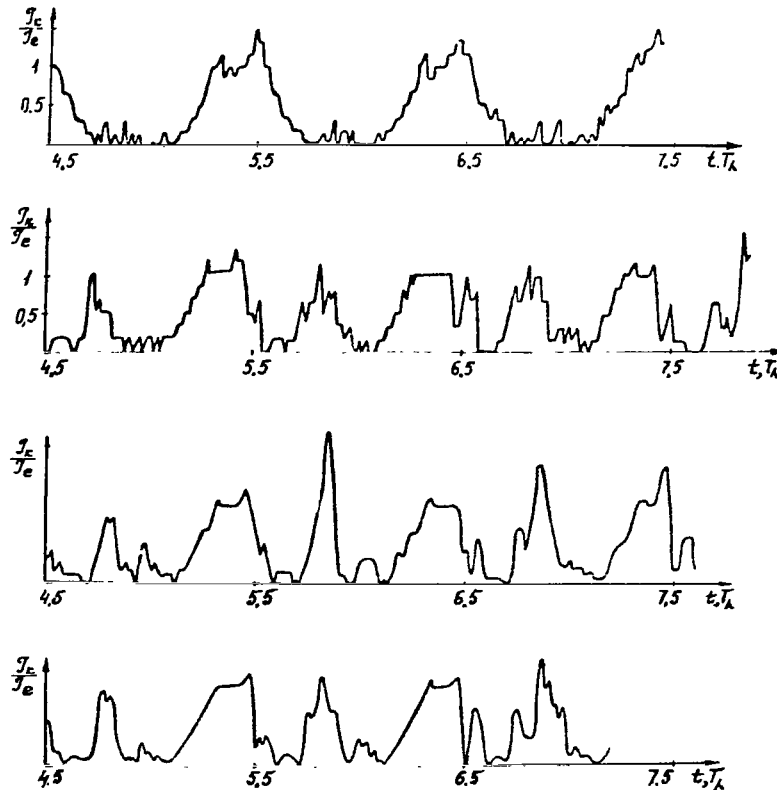


Figure 6. The Dependence of  $I_k/I_e$  on  $t$  for  $I_e = 5$  A for  
 $k = 6$ ,  $15 \times 30$  lattice;  $k = 6$ ,  $30 \times 60$  lattice;  $k = 12$ ,  $30 \times 60$   
lattice;  $k = 24$ ,  $30 \times 60$  lattice.

The equations of motion were integrated by the Runge-Kutta method, the Poisson equations — by the net-point method using the Seidel iteration method. The necessary analysis parameters are calculated. Satisfactory results are obtained for the simultaneous motion of 2000 particles and a calculation of the field from a  $30 \times 60$  lattice of points. Doubling the number of particles makes it possible to explain the more subtle effects in the current relationships. Calculations show that a consideration of the higher harmonics of the d-c and high-frequency field does not increase the volume of the analysis too drastically. This makes it possible to proceed to a study of actual double-row magnetron designs.

/18

#### REFERENCES

1. Yu, S. P., G. P. Kooper and O. Buneman. Time-Dependent Computer Analysis of Electron-Wave Interaction in Crossed Fields. *J. Appl. Phys.*, **36**, No. 8, 1965.
2. Kapitsa, P. L. *Elektronika bol'shikh moshnostey* (High-Power Electronics), Press of the Academy of Sciences USSR, Moscow, 1962.
3. Kapitsa, P. L., S. I. Filimonov and S. P. Kapitsa. Theory of Electron Processes in a Continuous-Operation Magnetron Oscillator. In coll.: *Elektronika bol'shikh moshnostey* (High-Power Electronics), Vol. 3, Nauka Press, Moscow, 1964.

4. Lomnev, S. P. Raschet i issledovaniye elektrofizicheskikh yavleniy na tsifrovyykh vychislitel'nykh mashinakh (The Analysis and Study of Electrophysical Phenomena on Digital Computers). VTs (Computer Center) Akad. Nauk SSSR, Moscow, 1965.

## INVESTIGATION OF THE PARTICLE-IN-CELL METHOD

/19

V. V. Yurchenko

**ABSTRACT:** This paper discusses light computational schemes of the PIC method, as applied to supersonic flow of a gas.

### 1. INTRODUCTION

In recent years, many papers have been written devoted to many variants of the method of "large particles" [1-5], in particular, for the solution of hydrodynamic problems by the particle-in-cell method [1, 4-8]. This method was tested by F. H. Harlow in 1957 [1], was published in a final edition in 1963 [7], and was further developed by co-workers at the Los Alamos Scientific Laboratory. During these years, he succeeded in solving numerous interesting physical problems. However, a detailed description of the method has not been openly published. Therefore, attempts to repeat the solution have encountered serious difficulties. The necessity has arisen for a more painstaking investigation of the particle-in-cell method in order to clarify its theoretical details.

### 2. DESCRIPTION OF THE METHOD

The particle-in-cell method is connected in a natural manner with various approaches to the solution of the hydrodynamic problems of Lagrange and Euler.

As we know, in Lagrange's representation, a liquid is partitioned at the initial instant of time into finite zones. Deformation of the network of zones in the course of time is connected with the motion of the liquid, which depends on a given numerical method for solving the differential equations of hydrodynamics. This technique exhibits a high degree of accuracy and is convenient for the solution of nonstationary problems. It enables one to follow the motion up to and including the fine structures of the flow. However, this approach has its defects, the most significant of which is its inapplicability in cases in which the medium undergoes strong deformations, large relative displacements, or is subject to other factors leading to a strong distortion of the original network.

/20

In Euler's representation, the liquid flows through a network of finite-difference cells that is fixed relative to a stationary (laboratory) system of coordinates. An important advantage of Euler's approach is the ability to calculate the motion of the liquid

under strong deformations and large relative displacements. But even this technique has a number of defects such as the difficulty of determining the fine structure of the flow, the difficulty of calculating the interfaces of the media, etc.

The particle-in-cell method is one of the attempts at combining these two different approaches, keeping the best characteristics of each. In calculations made with this method, the region of the solution is partitioned into Eulerian cells that are stationary with respect to the observer. One introduces a Lagrangian network of particles representing the elements of the fluid moving through the Eulerian network. The Eulerian network then describes the variable fields of flow and the Lagrangian network describes the parameters of the fluid itself. Obviously, the use of the two networks presents high requirements on the operating speed and memory of a computer. One should note the great graphic obviousness of the method, which is close to an analogy between the calculation and actual experiment (we impose initial and boundary conditions and then need only observe the development of the process). After each cycle, the result determines the real flow of the fluid at the corresponding instant of time. This fact points out the broad possibilities of the particle-in-cell method, especially in the solution of nonstationary problems with strong deformations of the flow.

In calculations made by the particle-in-cell method, the medium is represented in the form of discrete point masses, that is, particles moving through the Eulerian network. Here, the mass of an individual particle does not change. This makes it possible to eliminate from the complete system of hydrodynamic differential equations the equation of continuity, expressing the law of conservation of mass. Calculation of the change in the pattern of the motion of the medium involves time steps, or cycles. A cycle occupies a time interval  $\delta t$ . Each cycle is broken into two stages. The first stage involves the calculation of the flow of the fluid in Euler's representation. In this stage, the position of all particles is considered completely fixed. Therefore, in a system of equations describing the motion of an ideal fluid, the terms reflecting the displacement of the medium are omitted, and the system takes the following form

$$\frac{\partial \vec{V}}{\partial t} = -\frac{1}{\rho} \text{grad} P; \quad \frac{\partial I}{\partial t} = -\frac{P}{\rho} \text{div} \vec{V}, \quad (1)$$

where  $I$  is the specific internal energy of the medium. The result of the calculations at the Eulerian stage is the determination of the preliminary new values of  $\vec{V}$  and  $I$  at the end of a cycle. At the Lagrangian stage, one considers the motion of particles during the time  $\delta t$  of the same cycle. This stage takes into account the displacement of the medium. In the course of the motion, the particles transport their energy and momentum from one point in space to another. As a result of this redistribution of the masses, energies, and momenta, there will be a new change in the fields of the velocity and internal energy. The new values obtained for the fields of flow and the parameters of the fluid will describe a motion of the fluid at an instant of time corresponding to the end of the cycle.

At first glance, it may appear that the particle-in-cell method does not yield a stable solution since any solution of the system (1) other than that of undisturbed flow is explicitly unstable. However, as was shown in [8], the redistribution of the energy and momentum at the Lagrangian stage is equivalent to the addition of a number of terms in the equations of the system (1), some of these terms corresponding to the effective

viscosity and thermal conductivity. This explains the stability of the solutions obtained by the method.

### 3. THE BASIC COMPUTATIONAL FORMULAS

In the present article, the particle-in-cell method is applied to a specific problem of supersonic flow of an ideal gas around a cylinder, the axis of symmetry of which is directed along the incident flow. The region of the solution (see Fig. 1) is partitioned by means of a rectangular Eulerian network into  $I \times J$  cells. Since the problem is axis-symmetric, it reduces to the two-dimensional case, and the cells of the Eulerian network are annuli of rectangular cross-section. Each cell  $(i, j)$  is characterized by the following variables:

$u_{i, j}$ and $v_{i, j}$	-	the components of the rate of flow in the directions $z$ and $r$ ;
$M_{i, j}$	-	the mass of the gas in a cell;
$I_{i, j}$	-	the specific internal energy of the gas;
$P_{i, j}$	-	the pressure;
$E_{i, j}$	-	the total energy of the gas;
$Kz_{i, j}$ and $Kr_{i, j}$	-	the components of the momentum in the directions $z$ and $r$ .

/22

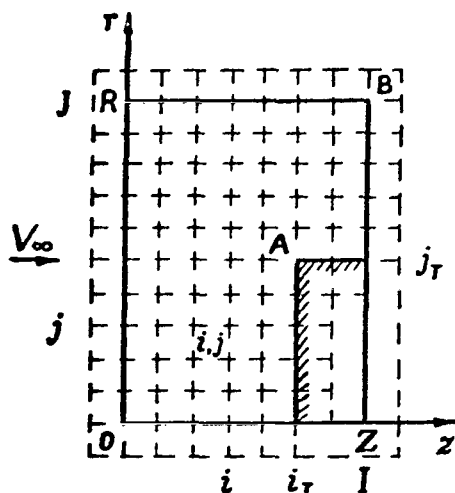


Figure 1. The Region of the Solution.

For each cycle, the initial conditions are the distribution of the particles and the values of the quantities  $M_{i, j}$ ,  $I_{i, j}$ ,  $u_{i, j}$ , and  $v_{i, j}$ , which are either determined in the preceding cycle or are given as initial conditions of the problem.

The system of equations (1) that describes the Eulerian stage of the calculation becomes, in cylindrical coordinates

$$\left. \begin{aligned} \frac{\partial u}{\partial t} &= -\frac{1}{\rho} \frac{\partial P}{\partial z}; & \frac{\partial v}{\partial t} &= -\frac{1}{\rho} \frac{\partial P}{\partial r}; \\ \frac{\partial I}{\partial t} &= -\frac{P}{\rho} \left[ \frac{\partial u}{\partial z} + \frac{1}{r} \frac{\partial(rv)}{\partial r} \right], \end{aligned} \right\} \quad (2)$$

or in finite-difference form

$$\frac{\tilde{u}_{i,j} - u_{i,j}}{\delta t} = -\frac{V_{i,j}}{M_{i,j}} \frac{P_{i+1,j} - P_{i-1,j}}{2\Delta z}; \quad (3)$$

$$\frac{\tilde{v}_{i,j} - v_{i,j}}{\delta t} = -\frac{V_{i,j}}{M_{i,j}} \frac{P_{i,j+1} - P_{i,j-1}}{2\Delta r}; \quad (4)$$

$$\frac{\tilde{I}_{i,j} - I_{i,j}}{\delta t} = -\frac{V_{i,j}}{M_{i,j}} P_{i,j} \left[ \frac{u_{i+1,j} - u_{i-1,j}}{2\Delta z} + \frac{v_{i,j+1} \left(j + \frac{1}{2}\right) - v_{i,j-1} \left(j - \frac{1}{2}\right)}{2\Delta r \left(j - \frac{1}{2}\right)} \right], \quad (5) \quad \text{/23}$$

where  $P_{i,j}$  is determined from the equation of state and  $V_{i,j}$  is the volume of the (i, j) cell.

When one specifies the boundary conditions for  $P$ ,  $u$ , and  $v$ , one completely determines the system (3) - (5). The solution of this system yields  $u_{i,j}$ ,  $v_{i,j}$ , and  $I_{i,j}$ . These are the tentative new values of the corresponding quantities. The boundary conditions are determined by the laws of conservation of the total energy of the system and the momentum. The question of the choice of boundary conditions will be examined in detail below. The Eulerian stage in the calculation ends with this.

Before turning to the Lagrangian stage, we need to carry out some supplementary operations. Specifically, we need to calculate the tentative total energy and momentum for each cell

$$\tilde{E}_{i,j} = M_{i,j} \left( \tilde{I}_{i,j} + \frac{\tilde{u}_{i,j}^2 + \tilde{v}_{i,j}^2}{2} \right); \quad \tilde{K}_{z,i,j} = M_{i,j} \tilde{u}_{i,j}; \quad \tilde{K}_{r,i,j} = M_{i,j} \tilde{v}_{i,j}. \quad (6)$$

At the Lagrangian stage, the displacement of particles is calculated in accordance with the values of  $u_{i,j}$  and  $v_{i,j}$  found during the cycle time  $\delta t$ . As a result of this



displacement, the coordinates of the particles change. Here, a particle can either remain in the same cell from which it began its motion, or shift to another cell, or completely leave the region of solution through the open boundary. Each k-particle that begins its motion in the cell (i, j) takes with it a mass  $m_k$  and (in proportion to that mass), an amount of momentum and energy:

$$K_z^{(k)} = m_k \tilde{u}_{i,j}; \quad K_r^{(k)} = m_k \tilde{v}_{i,j}; \quad E^{(k)} = m_k \left( \tilde{l}_{i,j} + \frac{\tilde{u}_{i,j}^2 + \tilde{v}_{i,j}^2}{2} \right). \quad (7)$$

Depending on where the particle is as a result of the displacement, the quantities  $Kz_{i,j}$ ,  $Kr_{i,j}$ ,  $E_{i,j}$  and  $M_{i,j}$  do not change if the particles do not cross the boundaries of the cell (i, j) and they decrease by an amount (7) if they do (in which case  $M_{i,j}$  changes accordingly). If the particle is in a new cell, then the quantities (7) and  $m_k$  are added to the corresponding quantities of that cell; if the particle leaves the region of solution, then (7) and  $m_k$  are "removed" from the system. With this redistribution of mass, energy, and momentum, the total change in them for the entire system is exactly equal to their flow through the open boundaries of the region of the solution. Integration of the motion of the particles can be done in various ways, which will be examined below. /24

As a result of the displacement of the particles of mass, the total energy and momentum in the cells assume, in general, new values

$$M'_{i,j}, \quad E'_{i,j}, \quad K'z_{i,j}, \quad K'r_{i,j}.$$

These values completely determine the field of flow at the end of a given cycle:

$$\left. \begin{aligned} u'_{i,j} &= \frac{K'z_{i,j}}{M'_{i,j}}; \quad v'_{i,j} = \frac{K'r_{i,j}}{M'_{i,j}}; \\ l'_{i,j} &= \frac{E'_{i,j}}{M'_{i,j}} - \frac{u'^2_{i,j} + v'^2_{i,j}}{2}. \end{aligned} \right\} \quad (8)$$

Thus, the values  $M'_{i,j}$ ,  $u'_{i,j}$ ,  $v'_{i,j}$  and  $l'_{i,j}$  obtained as a result of calculations in the Lagrangian stage constitute the solution of the problem for the corresponding instant of time and they serve as initial conditions for the following cycle.

#### 4. THE CHOICE OF BOUNDARY CONDITIONS

To specify the boundary conditions for the system (3) - (5), it is necessary to surround the entire boundary of the region of the solution with a number of fictitious cells as indicated in Fig. 1. The specification of P, u, and v in them will then completely determine the system.

Our region of solution has, as one can see from Fig. 1, the following boundaries, each with a differing in physical meaning:

OR, the incident flow, represented by the fictitious cells  $(0, j)$ , where  $j = 1, \dots, J$ ;

RB and  $Bj_T$ , the open boundary, represented respectively by the cells  $(i, J + 1)$ , where  $i = 1, \dots, I$ , and  $(I + 1, j)$ , where  $j = j_T + 1, \dots, J$ ;

$Oi_T$ , the axis of symmetry, represented by the cells  $(i, 0)$ , where  $i = 1, \dots, i_T$ ;

$Ai_T$ , the vertical boundary of the body, represented by the cells  $(i_T + 1, j)$ , where  $j = 1, \dots, j_T$ ; /25

$Aj_T$ , the horizontal boundary of the body, represented by the cells  $(i, j_T)$ , where  $i = i_T + 1, \dots, I$ .

Furthermore, during stabilization of the gas flow, cells may be formed that are not filled with the medium. The determination of the quantities  $P$ ,  $u$ , and  $v$  for such empty cells also calls for preliminary investigations.

As one can see from [3, 7, 8], we can specify conditions on the boundary and in an empty cell in various ways. One combination or another was used in the above analyses of the physical phenomena occurring in the flow at the boundaries of the region and in the vicinity of an empty cell. Then, the momentum and energy of the entire system were investigated. The results are given in [7, 8]. However, in these last communications, there remains some arbitrariness and contradiction in the choice of boundary conditions.

As a first approximation, we can obtain the conditions from an analysis of the momentum of the system and the total energy flow in the gas through the boundary of a cell. The change in the component of the momentum along the axis and the total energy of the gas in the cell  $(i, j)$  during time  $\delta t$  are then as follows:

$$\Delta Kz_{i,j} = M_{i,j} (\tilde{u}_{i,j} - u_{i,j});$$

$$\Delta E_{i,j} = M_{i,j} \left( \frac{\tilde{u}_{i,j}^2 + \tilde{v}_{i,j}^2}{2} + \tilde{I}_{i,j} - \frac{u_{i,j}^2 + v_{i,j}^2}{2} - I_{i,j} \right),$$

When we use equations (3) - (5), these equations take the forms

$$\Delta Kz_{i,j} = V_{i,j} \frac{\delta t}{2\Delta z} (P_{i-1,j} - P_{i+1,j}); \quad (9)$$

$$\begin{aligned}
\Delta E_{i,j} = & V_{i,j} \frac{\delta t}{\Delta z} \frac{1}{2} \left( P_{i-1,j} \frac{\tilde{u}_{i,j} + u_{i,j}}{2} + P_{i,j} u_{i-1,j} \right) - \\
& - V_{i,j} \frac{\delta t}{\Delta z} \frac{1}{2} \left( P_{i+1,j} \frac{\tilde{u}_{i,j} + u_{i,j}}{2} + P_{i,j} u_{i+1,j} \right) + \\
& + V_{i,j} \frac{\delta t}{\Delta r} \frac{1}{2} \left[ P_{i,j-1} \frac{\tilde{v}_{i,j} + v_{i,j}}{2} + P_{i,j} v_{i,j-1} \left( 1 - \frac{2}{2j-1} \right) \right] \\
& - V_{i,j} \frac{\delta t}{\Delta r} \frac{1}{2} \left[ P_{i,j+1} \frac{\tilde{v}_{i,j} + v_{i,j}}{2} + P_{i,j} v_{i,j+1} \left( 1 + \frac{2}{2j-1} \right) \right].
\end{aligned} \tag{10}$$

The expression (10) can be written

/26

$$\Delta E_{i,j} = F_I + F_{II} + F_{III} + F_{IV},$$

where  $F_I, \dots, F_{IV}$  are the total energy flows through the boundaries of the cell (i, j) (see Fig. 2):

$$F_I = \frac{1}{2} V_{i,j} \frac{\delta t}{\Delta z} \left( P_{i-1,j} \frac{\tilde{u}_{i,j} + u_{i,j}}{2} + P_{i,j} u_{i-1,j} \right); \tag{11a}$$

$$F_{II} = -\frac{1}{2} V_{i,j} \frac{\delta t}{\Delta z} \left( P_{i+1,j} \frac{\tilde{u}_{i,j} + u_{i,j}}{2} + P_{i,j} u_{i+1,j} \right); \tag{11b}$$

$$F_{III} = \frac{1}{2} V_{i,j} \frac{\delta t}{\Delta r} \left[ P_{i,j-1} \frac{\tilde{v}_{i,j} + v_{i,j}}{2} + P_{i,j} v_{i,j-1} \left( 1 - \frac{2}{2j-1} \right) \right]; \tag{11c}$$

$$F_{IV} = -\frac{1}{2} V_{i,j} \frac{\delta t}{\Delta r} \left[ P_{i,j+1} \frac{\tilde{v}_{i,j} + v_{i,j}}{2} + P_{i,j} v_{i,j+1} \left( 1 + \frac{2}{2j-1} \right) \right]. \tag{11d}$$

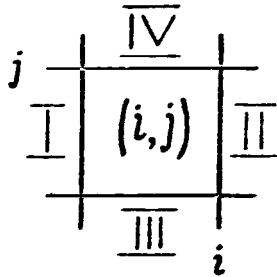


Figure 2. The Cell (i, j) in the Eulerian Network.

Since the boundary values of  $P$  for equations (3) and (4) and equation (5) can in general be different, we need to note that the pressure in Eq. (9) and in the left-hand terms of the expressions (11a) - (11d) is taken from the equation of motion (3) and that in the right-hand terms of (11a) - (11d) is taken from the energy equation (5).

Let us now look at the  $j$ th series of  $k$  cells  $(i, j), \dots, (i_k, j)$  and let us assume that cell  $(i, j)$  of this series is empty. Then, the total change in the momentum in these cells during time  $\delta t$  will be given by

$$\Delta K z_j = \sum_{i=i_1}^{i_k} \Delta K z_{i,j} = V_j \frac{\delta t}{\Delta z} \left( \frac{P_{i_1-1,j} + P_{i_1,j}}{2} - \frac{P_{i_k+1,j} + P_{i_k,j}}{2}, \frac{P_{l+1,j} - P_{l-1,j}}{2} \right). \quad (12)$$

The first two terms in (12) are equal to the impulse imparted to the medium in the above series of cells by the forces applied to the boundaries of that series. The last term is the undesirable extra impulse that the empty cell imparts to the medium. It vanishes under the condition

$$P_{l+1,j} = P_{l-1,j}. \quad (13)$$

Let us now look at two possible variations of the boundary conditions for different boundaries and an empty cell. /27

1. An empty cell. Suppose that cell  $(i, j)$  is empty. Since  $M_{i,j} = 0$ , the equations corresponding to that empty cell vanish from the system (3) - (5). The effect of the empty cell on the system can be eliminated by satisfying condition (13) and assuming that the energy flows into the empty cell from neighboring cells are equal to zero. This last condition is satisfied when the flows (11a) - (11d) for the cells adjacent to the empty one are equal to zero. Thus, we obtain the following system:

$$\begin{aligned} P_{i+1,j} &= P_{i-1,j}; \\ \hat{P}_{i,j} \frac{\tilde{u}_{i-1,j} + u_{i-1,j}}{2} + P_{i-1,j} u_{i,j} &= 0; \\ P_{i,j} \frac{\tilde{u}_{i+1,j} + u_{i+1,j}}{2} + P_{i+1,j} u_{i,j} &= 0; \\ P_{i,j} \frac{\tilde{v}_{i,j+1} + v_{i,j+1}}{2} + P_{i,j+1} v_{i,j} \left( 1 - \frac{2}{2j+1} \right) &= 0; \\ P_{i,j} \frac{\tilde{v}_{i,j-1} + v_{i,j-1}}{2} + P_{i,j-1} v_{i,j} \left( 1 + \frac{2}{2j-3} \right) &= 0. \end{aligned}$$

The solutions of this system yield all possible conditions eliminating the effect of the empty cell under the requirements mentioned above. These necessary conditions are as follows: for a solution of equation (3), it is necessary that

$$P_{i,j} = 0; \quad P_{i+1,j} = P_{i-1,j} = A, \quad (14)$$

where A is an arbitrary constant that can, in particular, be zero. Equation (4) can be solved under the unique condition

$$P_{i,j} = 0; \quad (15)$$

To solve equation (5), we need to satisfy only one of the following four combinations of conditions:

$$P_{i+1,j} = P_{i,j+1} = 0; \quad u_{i,j} = v_{i,j} = 0. \quad (16a, b)$$

$$P_{i+1,j} = v_{i,j} = 0; \quad P_{i,j+1} = u_{i,j} = 0. \quad (16c, d)$$

2. The incident flow. The boundary conditions for the fictitious cell (0, j) can be obtained from two considerations, namely, the constancy of the parameters of the incident flow or the constancy of the momentum imparted by that cell to the system and the constancy of energy flow through the boundary. In the first case, the boundary conditions for equations (3) and (5) have, respectively, the following forms:

$$P_{0,j} = P_{\infty}; \quad u_{0,j} = V_{\infty}. \quad (17)$$

In the second case, they can be obtained from the conditions of constancy of the momentum from (12) and the energy flow (11a):

$$\begin{aligned} V_j \frac{\delta t}{\Delta z} \frac{P_{0,j} + P_{1,j}}{2} &= V_j \frac{\delta t}{\Delta z} P_{\infty}; \\ \frac{1}{2} V_j \frac{\delta t}{\Delta z} \left( P_{0,j} \frac{\tilde{u}_{1,j} + u_{1,j}}{2} + P_{1,j} u_{0,j} \right) &= V_j \frac{\delta t}{\Delta z} P_{\infty} V_{\infty}. \end{aligned}$$

Solution of this system yields the boundary conditions for equations (3) and (5), respectively:

$$P_{0,j} = 2P_{\infty} - P_{1,j}; \quad (18a)$$

$$u_{0,j} = \frac{\tilde{u}_{1,j} + u_{1,j}}{2} + 2 \frac{P_{\infty}}{P_{1,j}} \left( V_{\infty} - \frac{\tilde{u}_{1,j} + u_{1,j}}{2} \right). \quad (18b)$$

3. The open boundary. Let us look at the case  $i = I$ . In analogy with what was done above, we can obtain the boundary conditions for equations (3) and (5) in the fictitious cell  $(I + 1, j)$  from an analysis of (12) and (11b). When we equate the second term in (12) to the momentum imparted by the external forces and equate the flow of energy (11b) through the boundary  $i = I$  to the flow of energy in the cell  $(I + 1, j)$ , we obtain the following system of equations for determining the boundary values of  $P$  and  $u$ :

$$V_j \frac{\delta t}{\Delta z} \left( \frac{P_{I+1,j} + P_{I,j}}{2} \right) = V_j \frac{\delta t}{\Delta z} P_{I+1,j}$$

$$\frac{1}{2} V_j \frac{\delta t}{\Delta z} \left( P_{I+1,j} \frac{\tilde{u}_{I,j} + u_{I,j}}{2} + P_{I,j} u_{I+1,j} \right) = V_j \frac{\delta t}{\Delta z} P_{I+1,j} u_{I+1,j}.$$

From this we obtain the desired boundary conditions for equations (3) and (5), respectively:

$$P_{I+1,j} = P_{I,j}; \quad (19a)$$

$$u_{I+1,j} = \frac{\tilde{u}_{I,j} + u_{I,j}}{2}. \quad (19b)$$

For the open boundary  $j = J$ , the flow of energy (11d) through that boundary can, in analogy with what was done above, be equated to the flow of energy in the cell  $(i, J + 1)$ , which yields the equation

/29

$$\pi \Delta z \delta t \left[ P_{i,J+1} \frac{\tilde{v}_{i,J} + v_{i,J}}{2} \left( R - \frac{\Delta r}{2} \right) + P_{i,J} v_{i,J+1} \left( R + \frac{\Delta r}{2} \right) \right] = 2 \pi \Delta z \delta t P_{i,J+1} v_{i,J+1} \left( R + \frac{\Delta r}{2} \right).$$

The solution of this equation yields the boundary conditions for equation (5) on the boundary  $i = J$ :

$$v_{i,J+1} = \frac{\tilde{v}_{i,J} + v_{i,J}}{2} \left( 1 + \frac{2}{2J+1} \right) \left( 2 - \frac{P_{i,J}}{P_{i,J+1}} \right)^{-1}, \quad (20)$$

where  $P_{i, j+1}$  are the boundary conditions for equation (4); in the present case, they are not determined.

4. Boundaries of the body. Let us look first at the vertical boundary  $i = i_T$ . In this case, the boundary conditions are taken under the assumption that the flow does impart or remove heat from the body. This means that the energy flow (11b) is equal to zero. Thus, we have the following equations

$$V_j \frac{\delta t}{\Delta z} \frac{P_{i_T, j} + P_{i_T+1, j}}{2} = V_j \frac{\delta t}{\Delta z} P_{i_T, j};$$

$$P_{i_T+1, j} \frac{\tilde{u}_{i_T, j} + u_{i_T, j}}{2} + P_{i_T, j} u_{i_T-1, j} = 0.$$

From this we get the boundary conditions for equations (3) and (5), respectively:

$$P_{i_T+1, j} = P_{i_T, j}; \quad (21a)$$

$$u_{i_T+1, j} = - \frac{\tilde{u}_{i_T, j} + u_{i_T, j}}{2}. \quad (22b)$$

To determine the conditions on the horizontal boundary of the body  $j = j_T$  from the same considerations, we equate the flow (11c) for the cell  $(i, j_T + 1)$  to zero and obtain

$$P_{i, j_T} \frac{\tilde{v}_{i, j_T+1} + v_{i, j_T+1}}{2} + P_{i, j_T+1} v_{i, j_T} \left( 1 - \frac{2}{2j_T+1} \right) = 0.$$

From this equation, the boundary conditions for the equation (5) on a horizontal rigid boundary assume the form

$$v_{i, j_T} = - \frac{\tilde{v}_{i, j_T+1} + v_{i, j_T+1}}{2} \left( 1 + \frac{2}{2j_T-1} \right) \frac{P_{i, j_T}}{P_{i, j_T+1}}, \quad (23)$$

where the  $P_{i, j_T}$  are the boundary conditions for equation (4). Their determination requires the use of supplementary considerations.

/30

5. The axis of symmetry. On the boundary  $j = 0$ , the flow behaves just as in the case of a rigid horizontal wall. Therefore, we can very simply use the results of section 4, which yield as boundary conditions for equation (5) on the axis of symmetry

$$v_{i,0} = \frac{\tilde{v}_{i,1} + v_{i,1}}{2} \frac{P_{i,0}}{P_{i,1}}, \quad (24)$$

where the  $P_{i,0}$  are the boundary conditions for equation (4), which require additional investigation.

Thus, we have found all the necessary boundary conditions for the system of equations (3) - (5). It should be noted that in the approximation of the equations of hydrodynamics by means of our system of finite-difference equations (3) - (5) with the boundary conditions (14), (18a), (19a), and (21a), the change in the momentum of the medium of the region in question is exactly equal to the momentum imparted by the forces acting on the boundaries of the region (we are considering the momentum and the change in momentum along the  $z$ -axis). This total change in momentum can be obtained by summing (12) with respect to  $j$ , taking into account the external forces that we specified a priori, when deriving the boundary conditions. This change will have the form

$$\Delta K_z = P_\infty \pi J^2 (\Delta r)^2 \delta t - \sum_{j=1}^{j_T} V_j \frac{\delta t}{\Delta z} P_{i_T, j} - \sum_{j=j_T+1}^J V_j \frac{\delta t}{\Delta z} P_{i, j}. \quad (25)$$

As we can see, the expression depends only on the external forces.

It follows from the law of conservation of energy that the change in the energy of a fluid in the region of solution under consideration during this time must be equal to the flow of energy through the boundary of the region. It is necessary to check whether or not this condition is satisfied for our approximating system of equations (3) - (5), with our boundary conditions. To investigate this, let us look at the three nonempty cells  $(i, j)$ ,  $(i-1, j)$ , and  $(i, j+1)$ . Obviously, this flow of energy from the cell  $(i-1, j)$  into the cell  $(i, j)$  must be equal to the flow of energy into the cell  $(i, j)$  from the cell  $(i-1, j)$ . This holds also for the cells  $(i, j)$ , and  $(i, j+1)$ . These two conditions can be written in the following form:

$$F_{1, i, j} = -F_{1, i-1, j} : F_{1, i, j+1} = -F_{1, i, j}, \quad (26)$$

where  $F_{1, i, j}$  is the flow  $F_1$  (see Fig. 2) for the cell  $(i, j)$ . If conditions (26) are satisfied, then, in the summation of  $\Delta E_{i, j}$  (10) over the whole region (which does not contain empty cells), the corresponding flows will cancel each other pair-wise and there will remain only flows of energy into the region through the external boundary; that is, the law of conservation of total energy will be satisfied. Conditions (26) for the system of equations (3) - (5) have the following forms:



$$P_{i-1,j}^{(3)} \frac{\tilde{u}_{i,j} + u_{i,j}^{(3)}}{2} + P_{i,j}^{(5)} u_{i-1,j}^{(5)} = P_{i,j}^{(3)} \frac{\tilde{u}_{i-1,j} + u_{i-1,j}^{(3)}}{2} + P_{i-1,j}^{(5)} u_{i,j}^{(5)}; \quad (27a)$$

$$\begin{aligned} P_{i,j}^{(4)} \frac{\tilde{v}_{i,j+1} + v_{i,j+1}^{(4)}}{2} \left( r_{j+1} - \frac{\Delta r}{2} \right) + P_{i,j+1}^{(5)} v_{i,j}^{(5)} \left( r_j - \frac{\Delta r}{2} \right) = \\ = P_{i,j+1}^{(4)} \frac{\tilde{v}_{i,j} + v_{i,j}^{(4)}}{2} \left( r_j - \frac{\Delta r}{2} \right) + P_{i,j}^{(5)} v_{i,j+1}^{(5)} \left( r_{j+1} + \frac{\Delta r}{2} \right), \end{aligned} \quad (27b)$$

where  $P_{i,j}^{(3)}$ , for example, denotes the pressure ascribed to cell (i, j) when equation (3) is solved. This partition is necessary since it is possible to ascribe various values of the parameters P, u, and v to a cell during the solution of the individual equations of the system (3) - (5) (as was done in the derivation of conditions (14) and (16a) - (16d)).

Equations (27a) and (27b) are valid, as one can easily see if and only if

$$\begin{aligned} P_{i-1,j}^{(3)} = P_{i-1,j}^{(5)}; \quad P_{i,j}^{(3)} = P_{i,j}^{(4)} = P_{i,j}^{(5)}; \quad P_{i,j+1}^{(4)} = P_{i,j+1}^{(5)}; \\ u_{i,j}^{(5)} = \frac{\tilde{u}_{i,j} + u_{i,j}^{(3)}}{2}; \quad u_{i-1,j}^{(5)} = \frac{\tilde{u}_{i-1,j} + u_{i-1,j}^{(3)}}{2}; \\ v_{i,j}^{(5)} = \frac{\tilde{v}_{i,j} + v_{i,j}^{(4)}}{2}; \quad v_{i,j+1}^{(5)} = \frac{\tilde{v}_{i,j+1} + v_{i,j+1}^{(4)}}{2}, \end{aligned}$$

Since (27a) and (27b) are written for any three cells, the preceding equations can be generalized as follows:

$$P_{i,j}^{(3)} = P_{i,j}^{(4)} = P_{i,j}^{(5)}; \quad (28a)$$

$$u_{i,j}^{(5)} = \frac{\tilde{u}_{i,j} + u_{i,j}^{(3)}}{2}; \quad v_{i,j}^{(5)} = \frac{\tilde{v}_{i,j} + v_{i,j}^{(4)}}{2}. \quad (28b)$$

Conditions (28a) and (28b) mean that, for exact conservation of the total energy, the parameters P, u, and v in an arbitrary interior cell of the region must correspond uniquely to that cell. Therefore, henceforth we shall not distinguish between them. It follows from condition (28b) that, in approximating the energy equation by means of the finite-difference equation (5), the law of conservation of energy cannot be satisfied.

Equation (5) must be replaced with

$$\begin{aligned} \frac{\tilde{I}_{i,j} - \dot{I}_{i,j}}{\delta t} = & - \frac{V_{i,j}}{M_{i,j}} P_{i,j} \left[ \frac{\hat{u}_{i+1,j} - \hat{u}_{i-1,j}}{2\Delta z} + \right. \\ & \left. + \frac{\hat{v}_{i,j+1} \left(j + \frac{1}{2}\right) - \hat{v}_{i,j-1} \left(j - \frac{3}{2}\right)}{2\Delta r \left(j - \frac{1}{2}\right)} \right], \end{aligned} \quad (29)$$

where

$$\hat{u}_{i,j} = \frac{\tilde{u}_{i,j} + u_{i,j}}{2}; \quad \hat{v}_{i,j} = \frac{\tilde{v}_{i,j} + v_{i,j}}{2}. \quad (30)$$

In this notation, the expressions (11a) - (11d) for the energy flows take the simpler forms

$$F_{I\ I,j} = \frac{1}{2} V_j \frac{\delta t}{\Delta z} (P_{i-1,j} \hat{u}_{i,j} + P_{i,j} \hat{u}_{i-1,j}); \quad (31a)$$

$$F_{II\ i,j} = -\frac{1}{2} V_j \frac{\delta t}{\Delta z} (P_{i+1,j} \hat{u}_{i,j} + P_{i,j} \hat{u}_{i+1,j}); \quad (31b)$$

$$F_{III\ i,j} = \frac{1}{2} \pi \Delta r \Delta z \delta t \left[ P_{i,j-1} \hat{v}_{i,j} \left(j - \frac{1}{2}\right) + P_{i,j} \hat{v}_{i,j-1} \left(j - \frac{3}{2}\right) \right]; \quad (31c)$$

$$F_{IV\ i,j} = -\frac{1}{2} \pi \Delta r \Delta z \delta t \left[ P_{i,j+1} \hat{v}_{i,j} \left(j + \frac{1}{2}\right) + P_{i,j} \hat{v}_{i,j+1} \left(j + \frac{3}{2}\right) \right]. \quad (31d)$$

We now find the boundary conditions for equations (3), (4), and (29) under which the momentum and total energy of the system are conserved.

6. An empty cell. Suppose that cell (i, j) is empty. Then, after summation of  $\Delta E_{i,j}$  over the entire region, the energy flows between the interior cells will cancel each other pairwise. In the empty cells (i, j) the flows of energy into the empty cell, which in the summation yield

$$F_{II\ i-1,j} + F_{I\ i+1,j} + F_{III\ i,j+1} + F_{IV\ i,j-1} =$$

remain uncompensated. If we make this fictitious energy flow equal to zero, we obtain the following equation for the conditions in an empty cell:

$$\begin{aligned}
& \frac{V_j}{\Delta Z} [P_{i,j} (\hat{u}_{i+1,j} - \hat{u}_{i-1,j}) + \hat{u}_{i,j} (P_{i+1,j} - P_{i-1,j})] + \\
& + \left[ \hat{v}_{i,j} \left( j - \frac{1}{2} \right) (P_{i,j+1} - P_{i,j-1}) + \right. \\
& \left. + P_{i,j} \left( \hat{v}_{i,j+1} \left( j + \frac{1}{2} \right) - \hat{v}_{i,j-1} \left( j - \frac{3}{2} \right) \right) \right] \pi \Delta r \Delta z = 0.
\end{aligned} \tag{32}$$

When we take account of Eq. (13) in Eq. (32), we obtain the following two variants of conditions in an empty cell when the total energy and momentum are conserved:

$$P_{i,j} = 0; \quad P_{i+1,j} = P_{i-1,j}; \quad P_{i,j+1} = P_{i,j-1}; \tag{33a}$$

Here,  $\hat{u}_{i,j}$  and  $\hat{v}_{i,j}$  can be arbitrary;

$$P_{i,j} = 0; \quad P_{i+1,j} = P_{i-1,j}; \quad \hat{v}_{i,j} = 0, \tag{33b}$$

Here,  $\hat{u}_{i,j}$  can be arbitrary.

If, in addition to condition (32), we require that the flow of energy into the empty cell from each adjacent cell be equal to zero, this imposes the supplementary requirements on the parameters of the flow in the empty cell:

$$\begin{aligned}
& P_{i,j} \hat{u}_{i-1,j} + P_{i-1,j} \hat{u}_{i,j} = 0; \\
& P_{i,j} \hat{u}_{i+1,j} + P_{i+1,j} \hat{u}_{i,j} = 0; \\
& P_{i,j} \hat{v}_{i,j-1} + P_{i,j-1} \hat{v}_{i,j} \left( 1 + \frac{2}{2j-3} \right) = 0; \\
& P_{i,j} \hat{v}_{i,j+1} + P_{i,j+1} \hat{v}_{i,j} \left( 1 - \frac{2}{2j+1} \right) = 0,
\end{aligned}$$

These give two more variants of the possible conditions in the empty cell:

$$P_{i,j} = P_{i+1,j} = P_{i,j+1} = 0; \tag{33c}$$

$$P_{i,j} = \hat{u}_{i,j} = \hat{v}_{i,j} = 0; \quad P_{i+1,j} = A, \tag{33d}$$

where  $A$  is an arbitrary number.

7. The incident flow. The boundary conditions in a fictitious cell (0, j) are obtained in analogy with (17) and (18a), (18b). From the condition of constancy of the incident flow

$$P_{0,j} = P_{\infty}; \quad \hat{u}_{0,j} = V_{\infty}, \quad (34)$$

and, from the condition of constancy of the momentum

$$\left. \begin{aligned} P_{0,j} &= 2P_{\infty} - P_{1,j}; \\ \hat{u}_{0,j} &= \hat{u}_{1,j} + 2 \frac{P_{\infty}}{P_{1,j}} (V_{\infty} - \hat{u}_{1,j}). \end{aligned} \right\} \quad (35) \quad \text{/34}$$

8. The open boundary. Conditions on the boundary  $i = I$  are obtained in a manner analogous to the way we obtained (19a, b). In the present case, they give the following expressions for  $P$  and  $u$  in the fictitious cells  $(I+1, j)$

$$P_{I+1,j} = P_{I,j}; \quad \hat{u}_{I+1,j} = \hat{u}_{I,j}, \quad (36)$$

for  $j = J$ , similar to (20), the boundary condition of equation (29) will be

$$\hat{v}_{i,j+1} = \hat{v}_{i,j} \left( 1 + \frac{2}{2j+1} \right) \left( 2 - \frac{P_{i,j}}{P_{i,j+1}} \right)^{-1}. \quad (37)$$

9. Boundary of the body. It is obvious from conditions (21) - (23) that, in the present case, the boundary conditions for equations (3) and (29) on  $i = i_T$  will be

$$P_{i_T+1,j} = P_{i_T,j}; \quad \hat{u}_{i_T+1,j} = -\hat{u}_{i_T,j}; \quad (38)$$

on  $j = j_T$ , the boundary conditions of equation (29) take the form

$$\hat{v}_{i,j_T} = -\hat{v}_{i,j_T+1} \left( 1 + \frac{2}{2j_T-1} \right) \frac{P_{i,j_T}}{P_{i,j_T+1}}, \quad (39)$$

where  $P_{i,j_T}$  is the boundary condition of equation (4), the choice of which shall be made later.

10. The axis of symmetry. In analogy with (24) the boundary condition of equation (29) on the boundary  $j = 0$  will be

$$\hat{v}_{i,0} = \hat{v}_{i,1} \frac{P_{i,0}}{P_{i,1}}, \quad (40)$$

where  $P_{i,0}$  is the as yet undetermined boundary value of  $P$  of equation (4).

Thus, we have looked at two distinct systems of finite-difference equations approximating the equations of hydrodynamics, and we have found the possible variants of the boundary conditions for these systems.

It should be noted that, in the approximation of the equations of hydrodynamics by means of the system (3) - (5) with the appropriate boundary conditions (14) - (24), the momentum of the fluid along the  $z$ -axis is conserved. The flows of energy in the region of an empty cell and on the boundaries of the region in question have a completely defined meaning. When one uses the approximating system (3), (4), (29), the total energy of the fluid is also conserved.

/35

We can remove any remaining ambiguity in the choice of the proper variant of boundary conditions (from the initially equally-likely possible variants found above) if we also investigate the physical phenomena in the vicinity of an empty cell and at the boundary of the region.

## 5. THE COMPUTATIONAL SCHEME

### 1. Choice of initial conditions of the problem.

Let us look at the initial conditions of the problem. They can be specified in different ways, depending on the process that we need to investigate. In the present article, we are primarily interested in investigating the method itself rather than any particular physical problem. Therefore, with an eye to saving machine time, we pose the problem in the following way: A cylinder that is motionless with respect to the medium under a specified pressure  $P_\infty$  and density  $\rho_\infty$  achieves instantaneously a velocity  $V_\infty$  along the axis of symmetry. In this problem, we observe the onset, development, and stabilization of a shock wave.

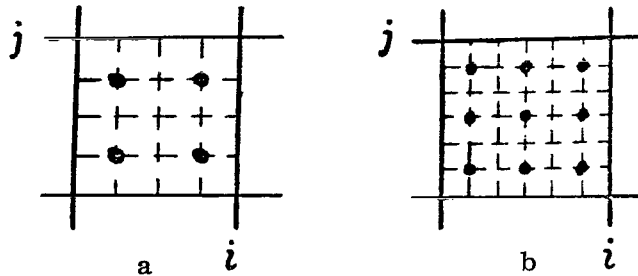


Figure 3. The Initial Distribution of Particles in the Cell: a)  $n = 2$ ; b)  $n = 3$ .

First of all, we choose the dimensions of the region of solution  $Z$  and  $R$  and the position of the cylinder in it. Keeping in mind the required accuracy of the solution and the possibilities of the computer, we then choose the Eulerian and Lagrangian networks. The dimensions of the Eulerian network are  $(I + 2) \times (J + 2)$  with consideration of the fictitious cells. The particles of the Lagrangian network at time  $= 0$  are distributed uniformly over the region. Therefore, it is convenient to put initially  $n^2$  particles into each cell  $(i, j)$ , where  $n = 1, 2, 3, \dots$ . Examples of such an initial distribution of the particles are shown in Fig. 3.

The initial conditions of the problem are as follows: a description of the particles (the  $k$ th particle has a definite mass  $m_k$  and coordinates  $z^{(k)}, r^{(k)}$ ) and a description of the Eulerian network [each cell  $(i, j)$  is characterized at time  $= 0$  by the quantities  $M_{i,j}, I_{i,j}, u_{i,j}$  and  $v_{i,j}$ ]. Since the density of the incident flow  $\rho_\infty$  is uniform, the  $m_k$  will depend, in the axisymmetric case, on  $r^{(k)}$ :

$$m_k = \frac{1}{n^2} 2 \rho_\infty \pi \Delta r \Delta z r^{(k)}; \quad (41a)$$

$$r^{(k)} = \frac{2Jn + 1 - 2k}{2n} \Delta r, \text{ where } k = 1, \dots, Jn; \quad (41b)$$

$$z^{(k)} = \frac{2I - 1}{2n} \Delta z, \text{ where } l = 1, \dots, In; \quad (41c)$$

where  $\Delta z = Z/I, \Delta r = R/J$ .

In the description of the Eulerian network,  $M_{i,j}$  is the sum of the masses of the particles in the cell  $(i, j)$ . Therefore, at time  $= 0$

$$M_{i,j} = 2 \rho_\infty \pi \Delta z (\Delta r)^2 \left( j - \frac{1}{2} \right). \quad (42)$$

The specific internal energy corresponding to the cell  $(i, j)$  at time  $= 0$  is determined from the equation of state of an ideal polytropic gas

$$I_{i,j} = \frac{P_\infty}{\rho_\infty (\gamma - 1)}. \quad (43)$$

The velocities in the cells conform to an undisturbed incident flow:

$$u_{i,j} = V_\infty; \quad v_{i,j} = 0. \quad (44)$$

Formulas (41) - (44) completely determine the initial conditions of the problem.

## 2. Description of the Computational Cycle.

1. Determination of the pressure. In the first step of each cycle, the pressure in each cell is determined from the initial values  $M_{i,j}$  and  $I_{i,j}$  which depend on the selected equations of state. In the present article, the equation of state was taken in the form /37

$$P = \rho I (\gamma - 1),$$

from which we get the pressure in cell  $(i, j)$ :

$$P_{i,j} = \frac{M_{i,j}}{V_{i,j}} I_{i,j} (\gamma - 1), \quad (45)$$

where  $V_{i,j}$  is the volume of the cell:

$$V_{i,j} = 2 \pi \Delta z (\Delta r)^2 \left( j - \frac{1}{2} \right). \quad (46)$$

We note that the pressure in an empty cell, which is found from Eq. (45) automatically vanishes. From these values  $P_{i,j}$  is determined in a neighborhood of an empty cell, and also in the fictitious boundary cells, from one of the variants of the boundary conditions (14) - (24) or (33) - (40), depending on the finite-difference equation that is chosen to approximate the energy equation.

2. Determination of the tentative new values of  $\tilde{u}$ ,  $\tilde{v}$ , and  $\tilde{I}$ . From the values  $P_{i,j}$  found in the preceding step, we determine the tentative new values of  $\tilde{u}_{i,j}$  and  $\tilde{v}_{i,j}$  in accordance with (3) and (4):

$$\tilde{u}_{i,j} = u_{i,j} - \frac{\pi \Delta z (\Delta r)^2 \left( j - \frac{1}{2} \right)}{M_{i,j}} (P_{i+1,j} - P_{i-1,j}) \delta t; \quad (47)$$

$$\tilde{v}_{i,j} = v_{i,j} - \frac{\pi \Delta z (\Delta r)^2 \left( j - \frac{1}{2} \right)}{M_{i,j}} (P_{i,j+1} - P_{i,j-1}) \delta t. \quad (48)$$

It should be noted that the pressure in the fictitious cell  $(i_T + 1, j)$  assumes different values in the calculation of  $\tilde{u}_{i_T, j_T}$  and  $\tilde{v}_{i_T + 1, j_T + 1}$ . In the first case, it is treated as the vertical boundary of the body and in the second as the horizontal boundary. For an empty cell,  $\tilde{u}_{i, j}$  and  $\tilde{v}_{i, j}$  have no meaning and can be arbitrary. For the sake of definiteness, they were taken equal to zero.

From the values of  $\tilde{u}_{i, j}$  and  $\tilde{v}_{i, j}$  that we have found, we determine the velocities in the fictitious boundary cells in accordance with one of the variants of the boundary conditions (16) - (24) or (33) - (40), after which we determine the new tentative values of  $\tilde{I}_{i, j}$  from (5) or (29). These yield, respectively

$$\begin{aligned} \tilde{I}_{i, j} = I_{i, j} - \delta t \pi \Delta z (\Delta r)^2 \left( j - \frac{1}{2} \right) \frac{P_{i, j}}{M_{i, j}} \left[ \frac{u_{i+1, j} - u_{i-1, j}}{\Delta z} + \right. \\ \left. + \frac{v_{i, j+1} \left( j + \frac{1}{2} \right) - v_{i, j-1} \left( j - \frac{3}{2} \right)}{\Delta r \left( j - \frac{1}{2} \right)} \right], \end{aligned} \quad (49a)$$

or

$$\begin{aligned} \tilde{I}_{i, j} = I_{i, j} - \delta t \pi \Delta z (\Delta r)^2 \left( j - \frac{1}{2} \right) \frac{P_{i, j}}{M_{i, j}} \left[ \frac{\hat{u}_{i+1, j} - \hat{u}_{i-1, j}}{\Delta z} + \right. \\ \left. + \frac{\hat{v}_{i, j+1} \left( j + \frac{1}{2} \right) - \hat{v}_{i, j-1} \left( j - \frac{3}{2} \right)}{\Delta r \left( j - \frac{1}{2} \right)} \right]. \end{aligned} \quad (49b)$$

In an empty cell,  $\tilde{I}_{i, j}$  is taken equal to zero. For cells inside the body, we cannot make calculations from (47) - (49) because of the instability of equations (2). The tentative new values of  $\tilde{E}_{i, j}$ ,  $\tilde{K}_z_{i, j}$ ,  $\tilde{K}_r_{i, j}$  are determined from (6) on the basis of the values found for  $\tilde{u}_{i, j}$ ,  $\tilde{v}_{i, j}$  and  $\tilde{I}_{i, j}$ .

**3. The motion of the particles.** At this step, we integrate the equations of motion of the particles. As calculations on a computer have shown, the integration does not require a high degree of accuracy and for it Euler's method is quite sufficient:

$$\left. \begin{aligned} z_q^{(k)} &= z_0^{(k)} + \sum_{q=1}^{n'} u_q \Delta \tau; \\ r_q^{(k)} &= r_0^{(k)} + \sum_{q=1}^{n'} v_q \Delta \tau, \end{aligned} \right\} \quad (50)$$



where  $\Delta \tau = \epsilon t / n'$  and  $\Delta \tau$  is the integration interval. The velocities  $u_q$  and  $v_q$  are determined by means of the velocity field  $\tilde{u}_{i,j}$  and  $\tilde{v}_{i,j}$ . The simplest procedure is to determine  $u_q$  and  $v_q$  only from the values of the velocities in the cell in which a particle is at a given instant, that is,

$$u_q = \tilde{u}_{i,j}; \quad v_q = \tilde{v}_{i,j}. \quad (51)$$

Here,

$$\Delta r(j-1) < r_q^{(k)} \leq \Delta r \cdot j; \quad \Delta z(i-1) < z_q^{(k)} \leq \Delta z \cdot i.$$

If a particle is in an empty cell, it continues to move with the velocity it had in the neighboring cell. If the particle impinges on a rigid wall, it is reflected from it and the collision is assumed to be completely elastic. As a consequence of the collision, the component  $u_q$  and  $v_q$  corresponding to it changes sign [the corresponding component  $\vec{K}^{(k)}$  in (7) also changes sign]. The axis of symmetry is now treated as a rigid wall. If the particle leaves the region, the integration is terminated and the characteristics of the particle  $m$ ,  $z$ , and  $r$  are not stored in the memory of the computer. /39

More accurate values of  $u_q$  and  $v_q$  can be obtained by linear interpolation of the values of  $\tilde{u}$  and  $\tilde{v}$  in the four cells closest to the particle. In this case, if

$$\Delta r \left( j - \frac{1}{2} \right) < r_q^{(k)} \leq \Delta r \left( j + \frac{1}{2} \right); \quad \Delta z \left( i - \frac{1}{2} \right) < z_q^{(k)} \leq \Delta z \left( i + \frac{1}{2} \right),$$

then, as one can see from Fig. 4,

$$u_q = u' + (u'' - u') \left[ \frac{z_q^{(k)}}{\Delta z} - \left( i - \frac{1}{2} \right) \right]; \quad (52a)$$

$$v_q = v' + (v'' - v') \left[ \frac{r_q^{(k)}}{\Delta r} - \left( j - \frac{1}{2} \right) \right], \quad (52b)$$

where

$$\begin{aligned}
u' &= \tilde{u}_{i,j} + A(\tilde{u}_{i,j+1} - \tilde{u}_{i,j}); \\
u'' &= \tilde{u}_{i+1,j} + A(\tilde{u}_{i+1,j+1} - \tilde{u}_{i+1,j}); \\
v' &= \tilde{v}_{i,j} + A(\tilde{v}_{i,j+1} - \tilde{v}_{i,j}); \\
v'' &= \tilde{v}_{i+1,j} + A(\tilde{v}_{i+1,j+1} - \tilde{v}_{i+1,j}),
\end{aligned}$$

where

$$A = \frac{r_q^{(k)}}{\Delta r} - \left(j - \frac{1}{2}\right).$$

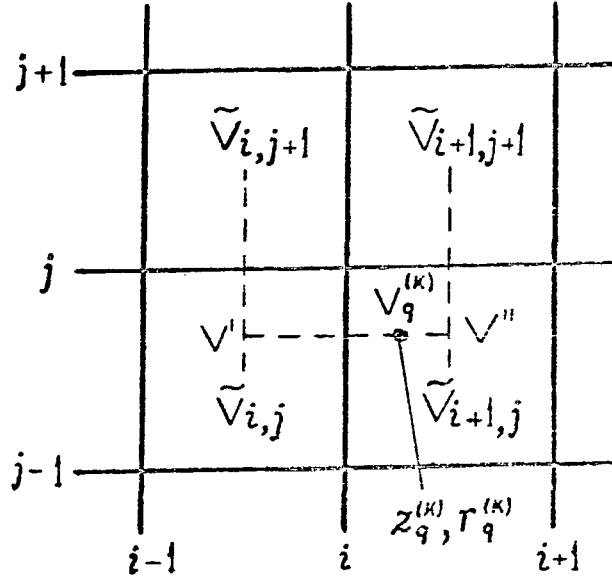


Figure 4. The Linear Interpolation of Velocities of a Particle (k).

If one or more of these four cells are empty, then the values  $\tilde{u}$  and  $\tilde{v}$  in them are taken equal to the corresponding values of  $u$  and  $v$  in the cell in which the particle is located at a given instant, or in which it was located at time = 0 if it is in an empty cell at the given instant. On the boundaries of the region of solution, we chose the following conditions:

If  $i = 0$ , then

$$\tilde{u}_{0,j} = \tilde{u}_{0,j+1} = V_\infty; \quad \tilde{v}_{0,j} = \tilde{v}_{0,j+1} = 0. \quad (53a)$$

For  $i = I$ ,

$$\left. \begin{aligned} \tilde{u}_{I+1, j} &= \tilde{u}_{I, j}; & \tilde{v}_{I+1, j} &= \tilde{v}_{I, j}; \\ \tilde{u}_{I+1, j+1} &= \tilde{u}_{I, j+1}; & \tilde{v}_{I+1, j+1} &= \tilde{v}_{I, j+1}. \end{aligned} \right\} \quad (53b)$$

At the upper open boundary  $j = J$ , we have analogously

$$\left. \begin{aligned} \tilde{u}_{i, J+1} &= \tilde{u}_{i, J}; & \tilde{v}_{i, J+1} &= \tilde{v}_{i, J}; \\ \tilde{u}_{i+1, J+1} &= \tilde{u}_{i+1, J}; & \tilde{v}_{i+1, J+1} &= \tilde{v}_{i+1, J}. \end{aligned} \right\} \quad (53c)$$

If the particle is close to the boundary of the body or close to the axis of symmetry, then the values of  $\tilde{u}$  and  $\tilde{v}$  in the fictitious boundary cells were chosen from the condition of impenetrability of the boundary, that is, from the condition that the normal component of the velocity vanishes on these boundaries. This condition was satisfied in the following way:

For  $i = i_T$ ,

$$\left. \begin{aligned} \tilde{u}_{i_T+1, j} &= -\tilde{u}_{i_T, j}; & \tilde{v}_{i_T+1, j} &= \tilde{v}_{i_T, j}; \\ \tilde{u}_{i_T+1, j+1} &= -\tilde{u}_{i_T, j+1}; & \tilde{v}_{i_T+1, j+1} &= \tilde{v}_{i_T, j+1}. \end{aligned} \right\} \quad (53d)$$

for  $j = j_T$ ,

$$\left. \begin{aligned} \tilde{u}_{i, j_T} &= \tilde{u}_{i, j_T+1}; & \tilde{v}_{i, j_T} &= -\tilde{v}_{i, j_T+1}; \\ \tilde{u}_{i+1, j_T} &= \tilde{u}_{i+1, j_T+1}; & \tilde{v}_{i+1, j_T} &= -\tilde{v}_{i+1, j_T+1}. \end{aligned} \right\} \quad (53e)$$

for  $j = 0$ , we have analogously

$$\left. \begin{aligned} \tilde{u}_{i, 0} &= \tilde{u}_{i, 1}; & \tilde{v}_{i, 0} &= -\tilde{v}_{i, 1}; \\ \tilde{u}_{i+1, 0} &= \tilde{u}_{i+1, 1}; & \tilde{v}_{i+1, 0} &= -\tilde{v}_{i+1, 1}. \end{aligned} \right\} \quad (53f)$$

If the particle began its motion in the cell  $(i, j)$  and after a time  $\delta t$  was in the cell  $(i', j')$ , then the values of  $m_k$  and (7) are taken from the values of  $M_{i, j}$ ,  $\tilde{K}z_{i, j}$ ,  $\tilde{K}r_{i, j}$  and  $\tilde{E}_{i, j}$  and they are added to the corresponding values in the cell  $(i', j')$ , or they are omitted from the subsequent solution when the particle leaves the region of the solution.

After the integration of the motion of all particles in the region in question, the entry of new particles through the boundary  $i = 0$  was simulated. This is done by the introduction of  $nJ$  particles with parameters (41a, b, c) with  $l = 1$  into the computational schemes. Each of these particles bears a mass  $m_k$  into the corresponding cell  $(1, j)$ . Also,

$$K_z^{(k)} = m_k V_\infty; \quad K_r^{(k)} = 0; \quad E^{(k)} = m_k \left( l_\infty + \frac{V_\infty^2}{2} \right).$$

The process of displacement of the particles and the redistribution of the mass, energy, and momentum between the cells of the Eulerian network is now terminated.

As a result of the cycle of calculations, the values found for  $M_{i,j}$  and also  $u'_{i,j}$ ,  $v'_{i,j}$ ,  $l'_{i,j}$  determined from (8) are the initial conditions for the next cycle. For empty cells, these quantities were taken equal to zero.

The length of the cycle  $\delta t$  was taken to be

$$\delta t = \frac{\Delta z}{n V_\infty}. \quad (54)$$

As was pointed out in [1], in calculations according to the particle-in-cell method does not require satisfaction of Courant's condition

$$|V_{max}| \delta t \ll \Delta x.$$

Furthermore, for very small  $\delta t$ , it is impossible to obtain a stable solution. The value of  $\delta t$  should now be chosen from the condition

$$|V_{max}| \delta t \sim \Delta x.$$

The calculations by means of the cycles described above were made prior to the stabilization of the shock. As was shown in [4], this occurs in the present problem after a time

$$t_{stab} \sim \frac{d}{a_\infty \sqrt{M_\infty}}, \quad (55a)$$

where  $d$  is the diameter of the cylinder,  $a_\infty$  is the velocity of sound in the incident flow, and  $M_\infty$  is the Mach number of the incident flow. The number of the cycles until the stabilization is

$$s_{\text{stab}} = 2n \cdot \frac{\Delta r}{\Delta z} j_T \sqrt{M_\infty}. \quad (55b)$$

However, as calculations have shown, after the stabilization of the flow, the values of its parameters in the cells continued to oscillate as a result of the fluctuation in the number of particles in the cells. Therefore, the values obtained for the individual cycle must not be regarded as the final result describing the stabilization flow. To smooth the oscillations in the values of the parameters of the flow, a simple averaging with respect to time was performed:

$$\bar{u}_{i,j}(s) = \frac{\sum_{s=s_{\text{stab}}}^s u'_{i,j}}{s - s_{\text{stab}}}, \quad (56)$$

and  $\bar{v}_{i,j}(s)$ ,  $\bar{M}_{i,j}(s)$ ,  $\bar{T}_{i,j}(s)$  are defined analogously. In the calculation of these quantities, the possibility arises of making an additional improvement in the convergence of the solution. In certain trial computations, after  $t_{\text{stab}}$  is attained, the average values of  $\bar{u}_{i,j}(s)$ ,  $\bar{v}_{i,j}(s)$  and  $\bar{T}_{i,j}(s)$  were taken as the initial values for cycle  $s + 1$ .

Let us now look at the distribution of the machine memory during the time of the calculations. The stored values of the parameters for each cell in the Eulerian network, at various stages of calculation of a single cycle, are shown in the following table:

TABLE

$M I u v$	-	the initial conditions of the cycle;
$M I u v P$	-	calculation of the pressure via Eq. (45) and the specification of its boundary values on the vertical boundaries of the region and of the body;
$M I u v P \tilde{u}$	-	calculation $\tilde{u}_{i,j}$ from Eq. (47);
$M I u v P \tilde{u}$	-	the specification of boundary values of the pressure on the horizontal boundaries of the region and of the body;
$M I u v P \tilde{u} \tilde{v}$	-	calculation of $\tilde{v}_{i,j}$ from Eq. (48);
$M I u v P \tilde{u} \tilde{v}$	-	the specification of boundary values of the velocities on all boundaries of the region;
$M \tilde{u} \tilde{v} I \tilde{u} \tilde{v}$	-	calculation of $\tilde{I}$ from (5) or (29);
$M \tilde{E} \tilde{K} z \tilde{K} r \tilde{I} \tilde{u} \tilde{v}$	-	calculation of $\tilde{E}_{i,j}$ and $\tilde{K}_{i,j}$ from (6);
$M' E' K'_z K'_r$	-	integration of the motion of the particles;
$M' I' u' v'$	-	calculation of the final result of a cycle via Eq. (8).

As indicated in the table, each cell of the Eulerian network is described by no more than seven parameters simultaneously, and each particle of the Lagrangian network is described by no more than three parameters. The total machine memory needed is approximately equal to

$$(I + 2)(J + 2)7 + 3\bar{n}IJ = IJ(7 + 3\bar{n}),$$

where  $\bar{n}$  is the average number of particles in a cell.

## 6. RESULTS OF CALCULATIONS

To make a comparison of the different variations in the method, we made several trial calculations. All the calculations were made on a BESM-6 computer. In all cases, we used the same region of solution (see Fig. 1) with the following parameters:  $R = 2m$ ;  $Z = 1.4m$ ; and  $I = 14$ ;  $J = 20$ ;  $i_T = 13$ ;  $j_T = 10$ .

The parameters of the incident flow were taken with the following values:  $\gamma = 1.4$ ;  $\rho_\infty = 0.132 \text{ kg} \cdot \text{sec}^2/\text{m}^4$ ;  $P_\infty = 10332 \text{ kg/m}^2$ ;  $V_\infty = 673 \text{ m/sec}$ . These figures correspond to supersonic flow around an object with  $\text{Mach} = 2.03$ .

The number of particles in a cell  $n^2$  at time  $t = 0$  is equal to 4. They are distributed in the cell as indicated in Fig. 3a. Let us assume that the flow stabilizes after  $s_{\text{stab}} = 100$  cycles. The calculation was carried out to the 200th cycle. After the 100th cycle, the results were averaged over time.

The undetermined boundary values of the pressure at the horizontal boundaries were taken in analogy with the vertical boundaries, that is,

$$\begin{aligned} P_{i, J+1} &= P_{i, J} && \text{under conditions (20) and (37);} \\ P_{i, j_T} &= P_{i, j_T+1} && \text{under conditions (23) and (39);} \\ P_{i, 0} &= P_{i, 1} && \text{under conditions (24) and (40).} \end{aligned} \quad (57)$$

In the trial solutions, the following questions were investigated: the development of a shock wave, the form of the stabilized shock wave in comparison with the experimental data of [9], the behavior of the field of flow after stabilization of the shock wave. /44

The shock wave was determined from the break in the streamlines and from the discontinuity in density. From the increase in the density, one can determine the cell through which a shock wave passes and one can determine its position in that cell by a linear interpolation from the values of  $\rho$  in neighboring cells. Thus, if the shock wave is in cell  $(i, j)$ , its coordinates were determined in the following way:

$$r = \Delta r \left( j - \frac{1}{2} \right); \quad z = \Delta z \left( i + \frac{\rho_{i+1,j} - \rho_{i,j}}{\rho_{i+1,j} - \rho_\infty} \right). \quad (58)$$

Investigation of the method was done according to the following schemes:

**Scheme 1.** In this computational scheme, the equation of the energy was taken in the form (5). For boundary conditions, we used  $P$ ,  $u$ , and  $v$ , as determined by (14), (16a), (17), and (19) - (24). The velocity of the particle was determined from (51) without the linear interpolation ( $n' = 5$  in (50)).

The development of a shock wave is shown in Fig. 5. Calculations have shown that even in the first steps there arises a back flow in front of the body. Because of this, the wave propagates rapidly along the flow. On the boundary of the collision of the forward and the back flows, there is a concentration of particles. The determination of  $u_q^{(k)}$  and  $v_q^{(k)}$  from (51) artificially retards the stabilization of the flow in front of the body and it leads to subsequent concentration of particles on the boundary between those cells in which the velocities are directed toward each other. From this boundary, the disturbances are distributed upward along the flow, as if bounced from a rigid wall. The shock wave at the 60th step leaves the region of the solution. During the same time, more empty cells appear in front of the body. This leads to high pressure gradients, as a result of which the particles achieve high velocities and, after several cycles, the flow pattern is completely distorted.

**Scheme 2.** In this computational scheme, an attempt was made to decrease the concentration of particles in the region of the shock wave, keeping unchanged the other computational equations of scheme 1. For this, the following restrictions were imposed on the velocities of the particles:

$$\tilde{u}_{i,j} \geq 0, \quad \tilde{v}_{i,i} \geq 0. \quad (59)$$

If, as a result of solving equations (3), and (4), one of the components of the velocity in the cell  $(i, j)$  turned out to be negative (for example, suppose that  $\tilde{u}_{i,j} < 0$ ), it was taken equal to zero. Here,  $\tilde{I}_{i,j}$  was increased by an amount  $M_{i,j} \tilde{u}_{i,j}^{1/2}$  in order to /45  
conserve the total energy of the gas in the cell.

The results of the calculation are shown in Fig. 6, where the dashed curve indicates the shock wave obtained experimentally in [9]. In this case, the disturbances are propagated upward along the flow more slowly. For  $s = 60$ , the shape of the shock wave is close to the experimental one. Up to  $s = 100$ , the wave remains in the same region but no stabilization occurs. The effect of imposition of the restrictions (59) which violate the condition of conservation of momentum along the  $z$ -axis, begins to be felt. In this computational scheme, neither momentum nor energy is conserved. Beginning with  $s = 60$ , the wave is deformed. It is shifted toward the body at the axis of symmetry. The entire front of the shock wave is then distorted. Its position for  $s = 100$  is shown in Fig. 6. With subsequent calculations, the shock wave continued to be adjacent to the body along the axis of symmetry whereas, along the boundary  $i = J$ , it is displaced slowly upward /46  
along the flow. With time, the flow pattern becomes more and more distorted. By the instant  $s = 80$ , the parameters of the flow behind the shock wave reach their stable values but the oscillations increase with the passage of time. The numbers in Fig. 6 indicate the deviations (in percentages) of the parameters of the field of flow from their average values at the corresponding points of the region of the solution.

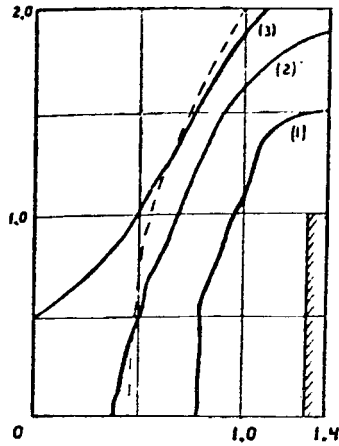


Figure 5. Results of the Calculation in Accordance with Scheme 1: - - - -, Position of the Shock Wave as Determined by Experiment in [9]; —, (1), (2), (3) the Position of the Shock Wave at Instants  $s = 20, 40, 60$ .

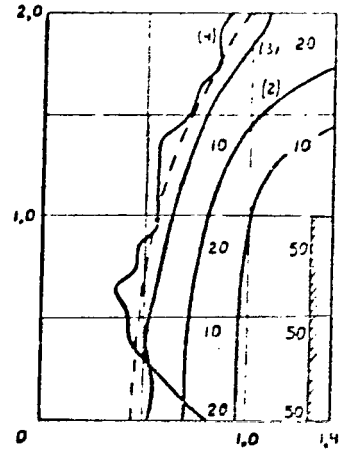


Figure 6. The results of Calculation According to Scheme 2: - - - -, Position of the Shock Wave as Determined by Experiment [9]; —, (1), (2), (3), (4) the Position of the Shock Wave for  $s = 20, 40, 60, 100$ .

**Scheme 3.** In contrast with the two preceding schemes, the total energy of the system is strictly conserved in the case of this scheme. This is done by taking the equation of the energy in the form (29) with boundary conditions (33c), (34), (36) - (40).

In this case, the shock wave develops even more slowly. It attains a stable position only by  $s = 80$ . Furthermore, just as with scheme 2, it begins to be deformed. Its position for  $s = 100$  is shown in Fig. 7. However, these deformations are insignificant and the shock wave remains at all times in a neighborhood of the experimental curve. The oscillations of the parameters of the flow behind the shock wave decrease to about one-half. The calculation time to the instant of stability of flow is 5 minutes.

**Scheme 4.** In this computational scheme, we investigated the influence of the method of determining  $u_q^{(k)}$  and  $v_q^{(k)}$ . All the equations and boundary conditions were the same as in scheme 1 except that we made a linear interpolation of the velocity from (52) instead of (51) in the calculation of the displacement of the particles. As before, we took  $n'$  in (50) equal to 5.

Just as in scheme 1, there again arises a back flow in front of the body. Up to the instant  $s = 100$ , the shock wave jets in the neighborhood of the experimental curve but, in contrast with the scheme 1, its position is stable. With subsequent calculations, the form of the shock wave is not deformed, and all the distortions that occur at  $s = 100$  are subsequently smoothed.



The results of the calculations are shown in Fig. 8. The position of the shock wave at  $s = 200$  was determined in accordance with (58) from the values of  $\rho$  averaged over the time. The values of the parameters of the flow behind the shock wave continue to oscillate around some average value even after stabilization. The oscillations of the averaged values are damped. Here, the average relative error far away from the body amounts to 3%, which is only half as large as in scheme 3. Directly in front of the body, these errors are significant, just as before (their values are shown in Fig. 8).

Scheme 5. In contrast with scheme 4, the equation of energy was taken here in the form (29) with boundary conditions (33c), (34), and (36) - (40).

/47

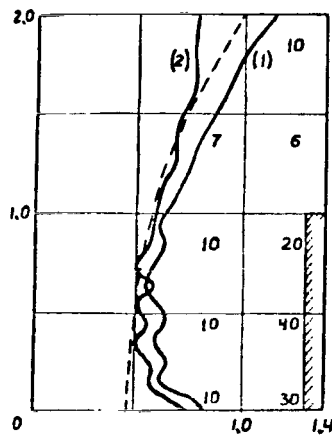


Figure 7. Scheme 3.

- - - -, Position of the Shock Wave as Indicated by Experiment in [9]; —, (1) Position of the Shock Wave for  $s = 100$ ; —, (2) the Shock Wave from the Density Values Averaged with Respect to Time from  $s = 100$  to  $s = 200$ .

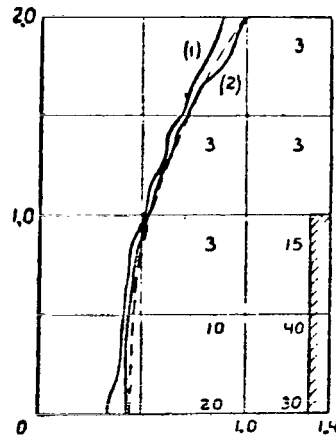


Figure 8. Scheme 4.

- - - -, the Shock Wave as Calculated from Experiment of [9]; —, (1) the Shock Wave for  $s = 100$ ; —, (2) the Shock Wave from the Averaged Values of  $\rho$  to the Instant  $s = 200$ .

The results of the calculations are shown in Fig. 9. With such an approximation of the energy equation, the shock wave sets in more slowly than in the scheme 4. By the instant  $s = 100$ , it still does not attain its stable position. The form of a shock wave found from the averaged values of the density  $s = 200$  coincides well with the experimental one (see Fig. 9). The oscillations of the parameters of the flow between the shock wave and the body decrease considerably.

An attempt was made to increase the accuracy of the calculation by decreasing the interval of integration of the equations of motion of the particles. Figure 10 shows the results of the calculations according to the same scheme but with  $n' = 10$ . The relative

deviations of the parameters of the flow from the corresponding average values between the shock wave and the body decreased somewhat. As before, the position of the shock wave coincides well with the experimental position. The time of calculation up to the instant of stabilization of the flow with the  $n' = 5$  amounted to 15 min and, for  $n' = 10$ , it amounted to 25 min.

/48

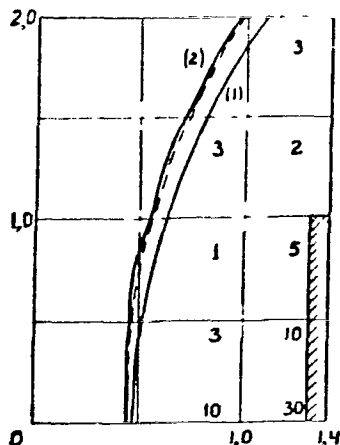


Figure 9. The Results of Calculation According to Scheme 5 with  $n' = 5$ : -----, the Shock Wave in [9]; —, (1) the Position of the Shock Wave for  $s = 100$ ; —, (2) the Position of the Shock Wave from the Averaged Values of  $\rho$  for  $s = 200$ .

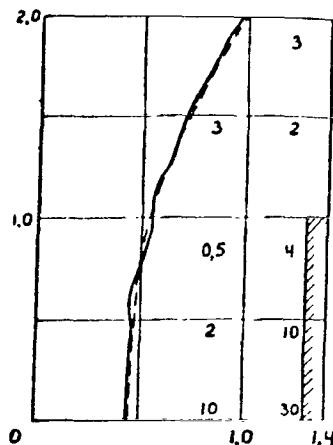


Figure 10. Scheme 5, with  $n' = 10$ : -----, the Shock Wave in the Experiment of [9]; —, the Shock Wave from the Averaged Values of  $\rho$  for  $s = 200$ .

**Scheme 6.** Several calculations were made according to scheme 5 but with the addition of the restriction (59).

The results of one such calculation are shown in Fig. 11. As it turned out, the restriction (59) was superfluous in schemes which included integration of the equations of motion of particles with linear interpolation of the velocity (52). Just as in schemes 2 and 3, there is a deformation of the shock wave. Again, it is displaced toward the body at the axis of symmetry and it moves upward along the flow by the boundary  $j = J$ . The oscillations of the parameters of the flow behind the shock wave are somewhat stronger than in scheme 5.

**Scheme 7.** Calculations in accordance with this scheme were made in accordance with the same equations and boundary conditions as in scheme 5. The initial number of particles in each cell was taken equal to  $n^2 = 9$  and they were distributed in the cell as indicated in Fig. 3b. Here, the time  $\delta t$  of a single cycle was accordingly decreased and

/49

the number of them increased. The flow stabilizes after  $s_{\text{stab}} = 150$ , and the calculation was carried out to  $s_{\text{final}} = 240$ . The time for calculation, in comparison with the calculation in accordance with scheme 5, increased by more than 300 %.

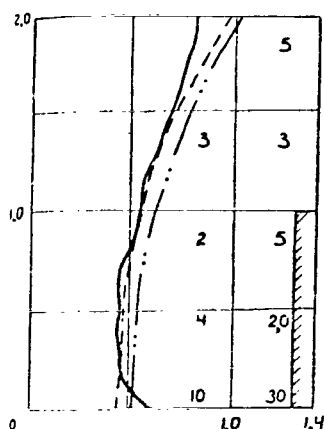


Figure 11. The Results of the Calculation in Accordance with Scheme 6: -----, the Experimental Position of the Shock Wave from [9], — . . — the Position of the Shock Wave for  $s = 100$ ; — the Shock Wave from the Averaged Values of  $\rho$  for  $s = 200$ .

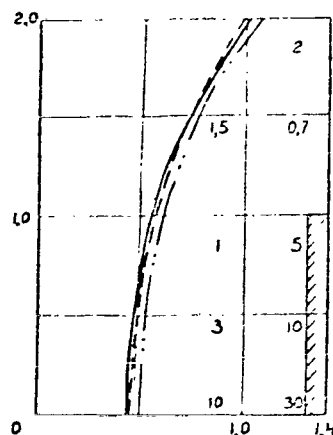


Figure 12. Calculation in Accordance with Scheme 7: -----, Experimental Position of the Shock Wave from [9]; — . . — the Shock Wave for  $s = 150$ ; — the Shock Wave from the Values of  $\rho$  Averaged over the Time for  $s = 240$ .

The results of the calculation are shown in Fig. 12. In comparison with the results of calculation via scheme 5, the improvements are insignificant. The position of the shock wave is again in good agreement with the experimental position. The deviations of the parameters of the flow decreased somewhat from their average values in the region between the shock wave and the open boundary  $i = I$ , and between the wave and the body they remained approximately the same. The time of calculation to stable flow amounted to 70 min.

**Scheme 8.** Calculations according to this scheme were carried out in the following way. Up to the instant of stabilization of the flow, the calculations were made according to scheme 5. Then, for every  $s > s_{\text{stab}}$ , the average values of  $\bar{u}_i(s)$ ,  $\bar{v}_i(s)$ , and  $\bar{I}_i(s)$  in (56) taken as initial conditions for the  $(s + 1)$  cycle. The equations and boundary conditions remained analogous to scheme 5.

The results of the calculations are shown in Fig. 13. The position of the shock wave is in good agreement with the experimental position. After  $s = 100$ , the solution rapidly

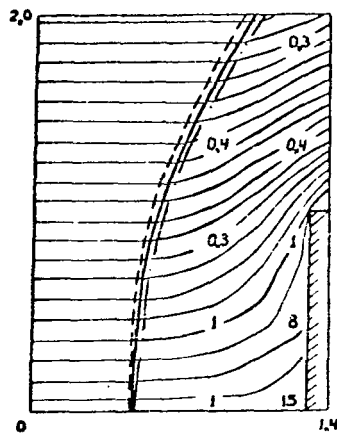


Figure 13. Scheme 8:  $M_{\infty} = 2.03$ : -----, the Shock Wave from Experiment [9]; - . . -, the Shock Wave for  $s = 100$ ; —, the Position of the Shock Wave from the Averaged Values of  $\rho$  for  $s = 200$ ; ———, the Streamlines Corresponding to the Instant  $s = 200$ .

converges. After 40 cycles, after stabilization of the flow, the deviation of the parameters from their averaged values does not exceed 1% over the entire region behind the shock wave except in a neighborhood of the stagnation point. Here, it should be noted that a significant increase in the accuracy for calculations in accordance with scheme 8 is achieved with hardly any increase in the calculating time. Figure 13 shows the streamlines corresponding to the time  $s = 200$ . The time of calculation to the instant of stable flow amounted to 10 min, and the total time of calculation amounted to 25 min.

To illustrate this scheme, we calculated the flow around a cylinder for  $M_{\infty} = 2.91$  and  $M_{\infty} = 4.35$ . In the first case, we set  $V_{\infty} = 966.3$  m/sec,  $i_T = 10$ ,  $s_{\text{stab}} = 200$ ,  $s_{\text{final}} = 320$ ; in the second case,  $V_{\infty} = 1444.0$  m/sec and  $i_T = 9$ .

The remaining initial and boundary conditions are analogous to the preceding case. The positions of the shock wave and the acoustic line obtained in the calculation according to scheme 8 for the given values of the Mach number are shown in Fig. 14.

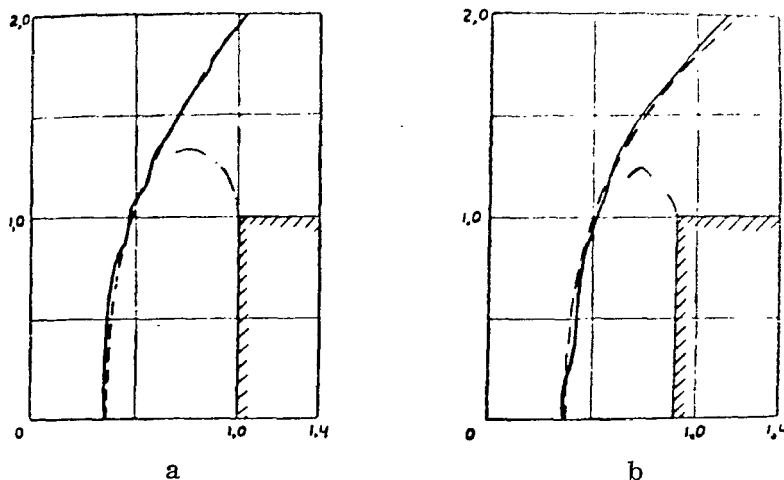


Figure 14. a)  $M_{\infty} = 2.91$ ; b)  $M_{\infty} = 4.35$ . The Results of the Calculation According to Scheme 8: ----- the Shock Wave from the Experiment of [9]; — the Calculated Shock Wave for  $s = 320$ ; - . . - the Acoustic Line.

## 7. CONCLUSION

The calculations according to all the schemes yield  $P_{1,j} = P_{\infty}$ . The boundary conditions (18a, b), (17) and (34), (35) coincide; that is, for supersonic flow, the conditions on the boundary  $i = 0$  have the form (17) or (34).

It is desirable that the value of the pressure be specified on the open boundaries more accurately since conditions (19a) and (36) yield values which are too high, and this distorts the flow in the neighborhood of the open boundaries. Therefore, the acoustic line left the region of the solution in all the calculations.

In comparing the computational schemes, we can draw the following conclusions:

1. Schemes 1 and 2 are not applicable for analysis of flows with great deformations.

2. Scheme 3 can be applied in the case of tentative calculations of nonstationary flows if great accuracy is not required. In the stationary case, it is sensible to carry out the solution only up to the instant of stabilization of the flow. This scheme can be used for nonstationary flows without great deformations when a slow computer with a sufficiently large memory is employed.

3. With calculations of nonstationary flow that require a specified degree of accuracy, we can use scheme 5. The decrease in the integration interval of the equations of motion of the particles produces an insignificant increase in the accuracy but a large increase in machine time. In this scheme, it is sufficient to choose  $n'$  between 3 - 6. In calculations of the flows involving subsequent compression of the medium, increase in the initial number of particles in a cell does not lead to a great increase in accuracy although, as one can see from the calculations, it does considerably increase machine time. The accuracy of calculations according to this scheme can be increased noticeably by decreasing the dimensions of the cell of the Eulerian network. In the case of calculations of flows with a fine structure or of region of special interest (for example, the neighborhood of a body), we can use locally a finer Eulerian network. Here, it is necessary to partition a particle entering this region into several smaller ones. It is probable that this will lead to an increase in the computational accuracy.

/52

4. For calculation of stationary axisymmetric flows, we can use scheme 8. All the remarks about the use of scheme 5 hold for this scheme. It should be noted that, for a more rapid convergence of the solution, it is necessary to determine the instant of stabilization of the flow as accurately as possible.

## REFERENCES

1. Harlow, F. H. Hydrodynamic problems involving large fluid distortions, *Journal of the Association for Computing Machinery*, April 1957, Vol. 4, No. 2.
2. Buneman, O. Dissipation of Currents in Ionized Media, *Phys. Rev.*, 1959, 115, No. 3.
3. Lomnev, S. P. Influence of Coulomb repulsion on the grouping of particles in a linear electron accelerator, *Doklady AN SSSR*, 1960, 135, No. 4.
4. Evans, M. W., and F. H. Harlow. Calculation of supersonic flow past an axially symmetric cylinder, *Journal of the Aeronautical Sciences*, April 1958, Vol. 25, No. 4.

5. Evans, M. W., and F. H. Harlow. Calculation of Unsteady Supersonic Flow Past a Circular Cylinder, ARS Journal, January 1959, Vol. 29, No. 1.
6. Evans, M. W., F. H. Harlow and B. D. Meixner. Interaction of Shock or Rarefaction with a Bubble, the Physics of Fluids, June 1962, Vol. 5, No. 6.
7. Harlow, F. H. The Particle-in-Cell Method for Numerical Solution of Problems in Fluid Dynamics, Experimental Arithmetics, High-Speed Computing and Mathematics, 1963, Vol. 15. /53
8. Computational Methods in Hydrodynamics, Moscow, Mir Press, 1967.
9. Maslennikov, V. G. On the Form of a Leaving Shock Wave Formed in the Case of Supersonic Motion of a Hemisphere and a Cylindrical Block in Various Gases; In the Collection: Aerofizicheskiye issledovaniya sverkhzvukovykh techeniy (Aerophysical Investigations of Supersonic Flows), Moscow, Nauka Press, 1967.

# SOME QUESTIONS IN THE CALCULATION OF THE EVOLUTION OF STARS

/54

S. N. Lomnev, K. A. Begishkina,  
Z. F. Levina, G. V. Ruben

ABSTRACT: Application of the hydrodynamic PIC method to the problem of evolution of stars is discussed.

For the past several years there has appeared in the literature a large number of articles devoted to calculation of the internal structure and gradual development of one-dimensional models of stars. The problem is formulated as a Cauchy problem for the system of equations

$$\left. \begin{aligned} \frac{\partial X}{\partial t} &= f_x(P, R, L, T, t); \\ \frac{\partial Y}{\partial t} &= f_y(P, R, L, T, t), \end{aligned} \right\} \quad (1)$$

describing the processes of nuclear transmutations of hydrogen and helium over time.

The internal structure of a star for fixed  $t$  is determined from the solution of the boundary value problem for the system of nonlinear ordinary differential equations

$$\left. \begin{aligned} \frac{dR}{dq} &= C_R R^{-2} \rho^{-1} \\ \frac{d\gamma}{dq} &= C_\rho R^{-4} q; \\ \frac{dL}{dq} &= C_L [C_{\epsilon_1} X^2 \rho T^4 + X(1-X-Y) \rho (C_{\epsilon_2} T^4)^4]; \\ \frac{dT}{dq} &= \frac{d \ln T_1}{d \ln P_1} \frac{dP}{dq}, \end{aligned} \right\} \quad (2)$$

where the  $C_i$  are constants and  $\rho$  is the density inside the star, which relate the variation of the radius  $R$ , the pressure  $P$ , the temperature  $T$  and the luminosity  $L$  with respect to the mass  $q$  of the star.

The basic difficulty is embodied in the solution of the boundary value problem. Earlier presented articles have been based on two methods: "trial integrations" (described by Schwartzschild [1]) and the double-sweep (proposed by Henyey, Levier et al. [2]).

The first uses a well known approach: the combination of trial integrals of (2) from two sides (from the surface and from the center of the model) with approximately given "missing" boundary conditions and calculation of corrections to these approximately given boundary conditions. To the disadvantages of the method one must ascribe the poor convergence of the corrections. Under the burning out of hydrogen in the center it is useless.

The double-sweep method offers the possibility of calculating the evolution of stars up to the late stages of burning of hydrogen and the onset of the burning of helium. However, using the linear approximation of the equations, we obtain a more precise value of the calculated quantities.

The difficulties of solution of two-dimensional problems and nonstationary processes of stars by these methods oblige one to seek new paths of research.

One of the possible processes of calculation of two-dimensional evolutionary problems can be the following. The system (2) is split into two subsystems, which are solved successively. In the capacity of the two "missing" functions are taken the values of the preceding model.

The first pair of equations will be expressions for the variation of  $P$  and  $R$ , the second pair for  $T$  and  $L$ . Such a choice of pairs of functions is illuminated by the fact that  $P$  or  $R$  characterize matter, and  $T$ ,  $L$  characterize the fields created by this matter. Thus, matter evokes variation of the fields, and the fields variation of matter. For a sufficiently fine step relative to  $t$  one should expect a sufficiently precise solution.

The splitting of (2) offers the possibility of using several schemes of calculation relative to  $t$ . The following appears interesting to us:

Scheme 1. At each step  $\Delta t$  one solves first the system for  $P$  and  $R$ . Then, not changing  $t$ , with the newly calculated  $R_1(q)$  and  $P_1(q)$  the system for  $L$  and  $T$  is integrated. The newly calculated  $L_1(q)$  and  $T_1(q)$  serve for the determination of  $R_2(q)$  and  $P_2(q)$  up until the  $(i+1)$ -th expressions do not differ from the  $i$ -th within a prescribed small magnitude.

Scheme 2. Pairs of equations are evenly divided with respect to time: in the odd steps  $R$ ,  $P$  are calculated, in the even  $L$ ,  $T$ .

Scheme 3. For fixed  $t$  the system for  $R$  and  $P$  is first solved. The calculated values are used in the integration of the equations for  $L$  and  $T$ .

Test calculations of the evolution of one-dimensional models stars were carried out. The best results were obtained with the use of scheme 2. Thus, on the time interval 0-10 years agreement was obtained with the magnitudes, calculated by another method, of 4-5 symbols.



Utilization of splitting of the equations appears advantageous to us in the later stages of evolution, for example, in time intervals where the Schwartzschild method converges poorly.

One-dimensional stationary processes with scales of phenomena of  $10^6$  give certain averaged characteristics of the development of stars. Hydrodynamic instabilities and two-dimensional phenomena (with scales of about a year and less) are more advantageously interpreted by means of "coarse particles". This offers a series of advantages.

1. The system of equations is simplified and is decomposed into two groups of equations which are sequentially solvable.

2. The equation of continuity, which is unstable for numerical solution, drops out and is replaced by a Cauchy problem for a system of ordinary differential equations.

Strong deformations of matter are permitted and, naturally, the physical process is described.

In this paper two versions of the method of "coarse particles" are employed: the method of "mean density" [3] and the method of "particles-in-cells" [4] (PIC for short). For exhibiting the particulars of the calculation the method is tested on a spherically symmetric star.

The "mean density" method. The radius of the star is divided into  $N$  intervals (cells with indices  $i = 1, 2, \dots, N$ ). The mass of each cell is decomposed into  $l$  particles. The calculation is begun by the determination of the density from the distribution among the cells. From the equation of state for the density the pressure

$$P_i = \frac{C_1 \rho T}{\mu} + (C_2 T)^4, \quad (3)$$

is obtained, where  $\mu$  is the mass of the  $i$ -th molecule,  $C_1, C_2$  are constants; the quantities  $\rho_i$  and  $P_i$  relate to the center of the  $i$ -th cell.

The next step consists in the integration of the field equations

$$\left. \begin{aligned} \frac{\partial L}{\partial r} &= 2 \pi r^2 \rho (\varepsilon - \varepsilon_G)_i \\ \frac{\partial T}{\partial r} &= - \frac{\partial \ln T}{\partial \ln P} \cdot \frac{GM \rho}{r^2}, \end{aligned} \right\} \quad (4)$$

where  $\varepsilon$  is the energy of burning,  $\varepsilon_G$  is the energy of contraction or expansion,

$M = \int_0^r 4 \pi r^2 \rho dV$ ,  $G$  is the gravitational constant, with the boundary conditions

/57

$$\left. \begin{aligned} L(0, t) &= 0; \\ T(r_*, t) &= L^{1/2}(r_*, t) r_*^{-1/2} T_{eff\odot} \end{aligned} \right\} \quad (5)$$

where  $T_{eff}$  is a constant.

The system (4), (5) is solved with the aid of trial integrations from both ends and determination of corrections at the point of joining. In the calculated fields motion of the particles takes place according to the equations

$$\frac{dr}{dt} = u; \quad \frac{du}{dt} = -\frac{1}{\rho} \frac{\partial P}{\partial r} - \frac{GM}{r^2}. \quad (6)$$

The system (6) was integrated by Euler's method. The gravitational force  $GM/r^2$  was determined relative to particles, the pressure gradient  $\frac{\partial P}{\partial r}/\rho$  relative to cells.

The form of the initial values  $u_i(0)$  and  $r_i(0)$  depends on the concrete problem.

Thus, calculation of the evolution of a star on the time interval  $T = \sum_{m=1}^M \Delta t_m$  consists of calculation of the field from (4), (5) for fixed  $t$  and shifting the masses (6) in these fields by  $\Delta t_m$ , wherein  $\Delta t_m$  is selected in accord with the condition of prohibition of transition of particles between cells  $\delta r_i \geq u_i \Delta t_m$ .

The distribution of particles and cells appears to be a complex problem and depends on a series of causes. Substantial difficulty resides in the sharp drop in density and pressure, changing by approximately 10 orders of magnitude from the center to the surface.

In this article two forms of the distributions of particles and cells were used:

a) the particles were of the same mass and were distributed proportionally to the initial density. The cells were taken such that into the first one four particles fell. Thus, on the surface and at the center of the star large cells were obtained;

b) particles and cells were distributed from the condition of small relative variations of the quantities of the field and pressure of the initial uniform model; 2000 particles of various masses were placed in 200 cells (10 in each). Thus, cells were obtained which were small at the center, increased toward the middle portion, and then again decreased toward the surface.

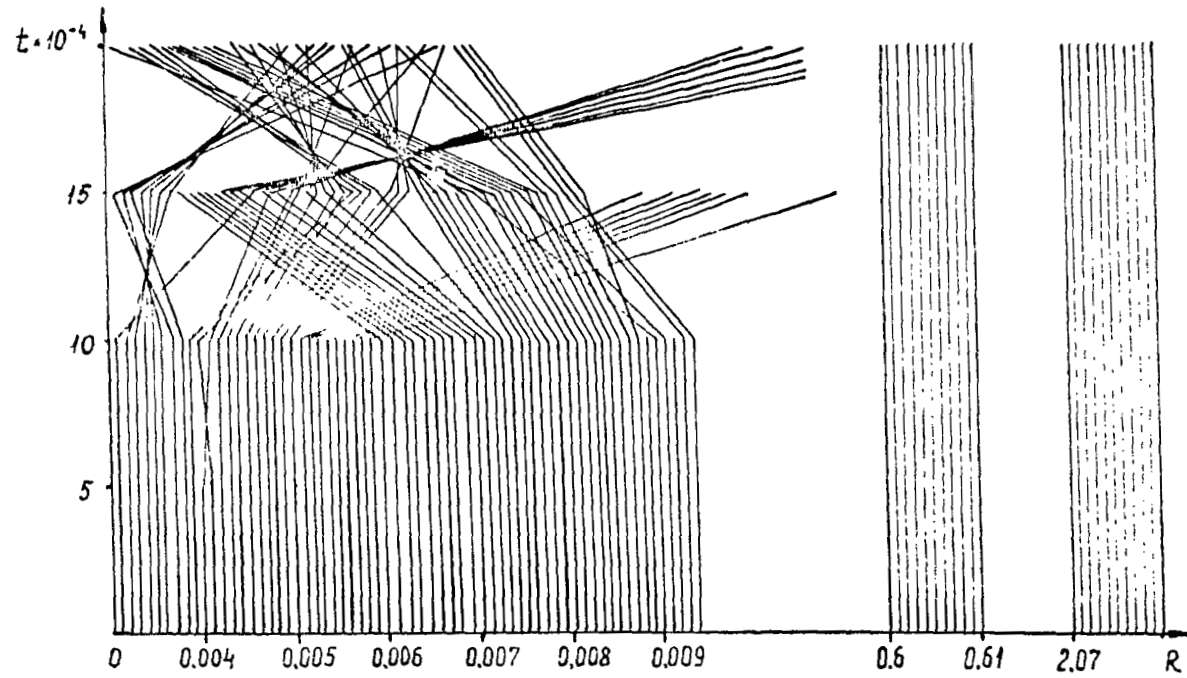


Figure 1. Trajectories of Particles near the Center.

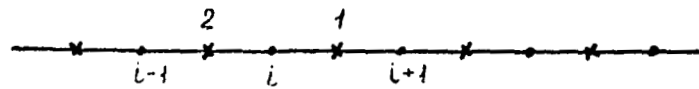


Figure 2. The Scheme of Distribution of Cells.

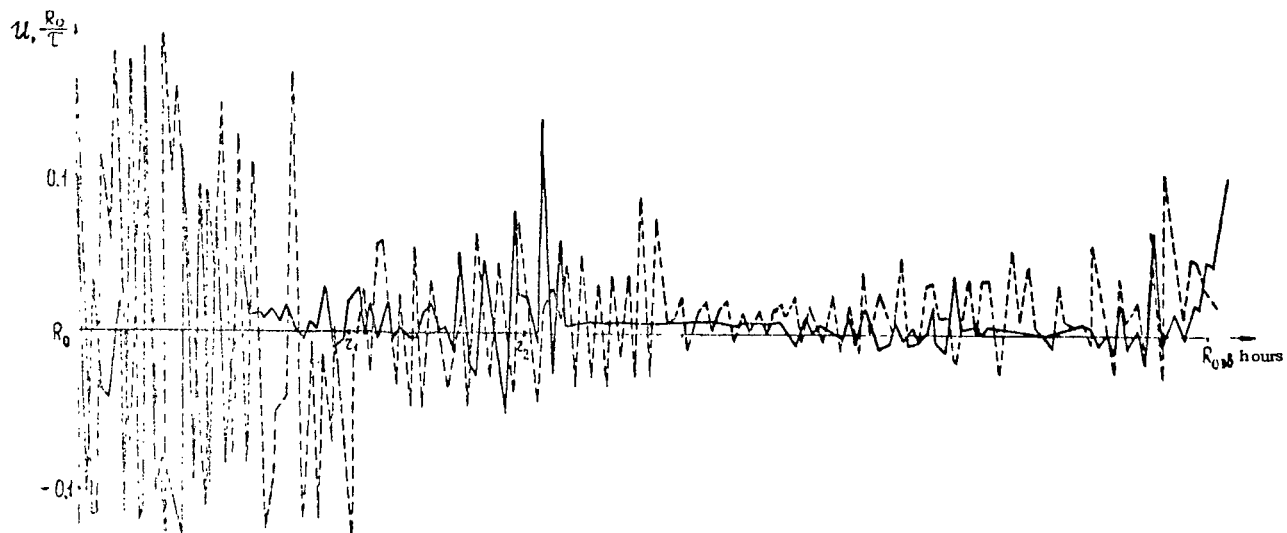


Figure 3. The Dependency  $u(r)$  at the times  $T_2$  and  $T_1$ ;  $R_0 = R_0 \cdot 3^{b/4}$ ;  $T_1 = 153\Delta t$ ;  $T_2 = 313\Delta t$ ;  $\Delta t = 0.0005$  hours ———  $153\Delta t$ ; - - - - -  $313\Delta t$ .

These two forms of the distributions were used in the calculations. The second type of distribution of particles and cells gave more stable results of the calculations.

/60

A series of general deficiencies were revealed.

1. In view of the constancy of the pressure gradient within a cell there are no collisions between particles. Hence particles of a cell move together and coagulation is obtained. (Fig. 1).

2. Small displacements of particles produce large variations of their velocity, and at each step they are accumulated. Attempts to smooth the pressure gradient and thereby decrease the scatter of the quantities did not permit complete removal of computational instabilities.

The method of "particles in cells" [4]. The deficiencies of the "mean density" method necessitated turning to the method of "particles in cells", which is used in certain complex nonstationary problems of hydrodynamics. Matter is divided into a large number of "coarse particles" (Lagrangian mesh), which move like points, having a given mass, across cells (Eulerian mesh). The density of matter in a cell is equal to the ratio of the mass of all the particles found in it to its volume. It is constant within a cell and changes stepwise between neighboring cells. The field quantities (i.e., temperature, energy flow, etc.) are also constant within a cell and are determined from difference equations. Solution of the problem leads to a series of steps according to time. Each step consists of three stages: calculation of the field quantities, movement of the particles and, finally, corrections of the field.

Calculations carried out by Harlow and others have shown that the method is expedient for problems in which large fluid deformations and large relative displacements are encountered, and impingement of the surfaces of separation of media arises.

In the problem considered there must not be regions of flow with small subsonic velocities. Inside large regions of flow there must not be encountered small regions in which it is necessary to know the solution in detail. We undertake to apply the scheme of the PIC method for the calculation of fast processes in the interiors of stars.

We shall consider the adiabatic case. We separate the star into  $N$  spherical zones identical in radial dimension (Fig. 2). In the first stage the fields are calculated according to the equations

$$m_i \frac{\bar{u}_i - u_i}{\Delta t} = -G \frac{M_i m_i}{r_i^2} - 4\pi r_i^2 \left( P_{i+\frac{1}{2}} - P_{i-\frac{1}{2}} \right); \quad (7)$$

$$\frac{\bar{Q}_i - Q_i}{\Delta t} = -4\pi P_i \left[ (r^2 \bar{u})_{i+\frac{1}{2}} - (r^2 \bar{u})_{i-\frac{1}{2}} \right], \quad i = 1, 2, \dots, N,$$

/61

here  $m_i$  is the mass of the  $i$ -th cell,  $u_i$  is the velocity,  $P_i$  the pressure,  $Q_i$  the internal energy, and  $V_i = 4\pi r_i^2 \delta r_i$  is the volume of the  $i$ -th cell, and  $\sim$  denotes the results after the first stage

$$\bar{u}_i = \frac{u_i + \tilde{u}_i}{2}; \quad P_{i+\frac{1}{2}} = \frac{P_{i+1} + P_i}{2}; \quad P_{i-\frac{1}{2}} = \frac{P_i + P_{i-1}}{2};$$

$$\bar{u}_{i+\frac{1}{2}} = \frac{\bar{u}_i + \bar{u}_{i+1}}{2}; \quad \bar{u}_{i-\frac{1}{2}} = \frac{\bar{u}_i + \bar{u}_{i-1}}{2}; \quad \tilde{E}_i = \tilde{Q}_i + \frac{m_i \tilde{u}_i^2}{2}.$$

The boundary conditions are obtained from the laws of conservation of energy

$$\bar{u}_{N+1} = 0; \quad P_{N+1} = 0;$$

$$2\pi[P_n (r^2 \bar{u})_{n-1} + P_{n-1} (r^2 \bar{u})_n] = 0,$$

where N is the last cell on the surface.

For  $n = 1$ , i.e. at the center, this equality is satisfied out of symmetry. In empty cells the pressure and velocity are equal to zero.

Initial conditions are taken from the results of calculation of the initial uniform model. The star was divided into 200 cells identical in dimension which were fixed, and to them were added another 100 empty cells. In each cell were distributed uniformly 10 particles of like mass for a given cell.

Partition into identical cells is advantageous for calculation and insures fulfillment of the law of conservation of energy, although it is crude for the surface, and in a central cell in the calculation of volume by the formula  $V_i = 4\pi r_i^2 \delta r_i$  the relative error amounts to 25%.

In the second stage particles move with velocities obtained by linear interpolation on the centers of two neighboring cells

$$\tilde{r}_k = r_k + v_k \Delta t,$$

here  $r_k, \tilde{r}_k$  are the coordinates of the particle before and after the movement,  $v_k$  is the velocity of the particle.

Trial calculations showed significant improvement of stability of the scheme in comparison with the case where the particle velocity was taken equal to the value at the center of the cell.

The Eulerian quantities are not altered if a particle does not transgress the boundary of a cell. In the contrary case the change is determined by addition and subtraction of masses, energies (kinetic heat advantage) and the amount of movement with the corresponding quantities by a given particle. The amount of movement of the particles is  $\tilde{Y}_k = m_k \tilde{u}_i$ , the energy is  $\tilde{E}_k = \tilde{E}_i m_k / m_i$ , where  $m_i, u_i$  and  $E_i$  are the parameters of the old cell after the first stage. In the third stage the corrections of the

field are calculated. After the movement of the particles we have  $Y_i'$ ,  $E_i'$ ,  $m_i'$  as the impulse, energy and mass of the  $i$ -th cell. We calculate

$$u_i' = \frac{Y_i'}{m_i'}; \quad Q_i' = E_i' - \frac{m_i' u_i'^2}{2}; \quad T_i'; \quad P_i'; \quad \rho_i'$$

for the  $i$ -th cell. These values are taken as the initial data for the next step of the calculations.

The masses of particles at the center and on the surface differ by 7 orders of magnitude. The feasibilities of the machine do not permit smoothing this difference completely; hence the calculations have a trial methodological character. An attempt to calculate pulsations of stars did not give good results; the method is too coarse for small pulsation velocities. The errors arising under sufficiently large time of computation exceed by far the given initial velocities. In the equilibrium model under consideration with zero initial velocities a velocity of movement arises and increases as a result of errors. In central cells the parameters are agitated in the first steps of the calculation. It is necessary to decrease substantially the time step or to throw out the  $n$  central cells. Discarding the center, the boundary conditions

$$P_n = P_{n+1}; \quad P_{n+\frac{1}{2}} = P_{n+1}; \quad \bar{u}_n = 0; \quad \bar{u}_{n+\frac{1}{2}} = \frac{\bar{u}_{n+1}}{2}.$$

were introduced. Particles are elastically reflected from the boundary of cells  $n$  and  $n+1$ . With the increase of  $n$  the time step required for the calculation increases, for  $n=50$ ,  $\Delta t = 0.0005$  hours, for  $n=155$ ,  $\Delta t = 0.005$  hours. For  $n=50$  after 153 steps it turns out that the greatest velocities occur in the central cells, at the surface, and in the neighborhood of  $r_1$ ,  $r_2$  (Fig. 3). Up to this moment of the calculation the density has not changed, except the density of certain cells at the center and at the surface. Thus, the velocity characterizes instability in the first step of the calculation.

An attempt to improve the accuracy by breaking down the cells for that same quantity of particles (they took  $N=400$  and 2000 particles) led to poorer results (Fig. 4). The pattern is particularly unstable in the neighborhood of  $R_0$ . In the remaining cells the results do not differ significantly in absolute value from the results for  $N=200$ . In Fig. 5 are presented the values of the velocity for  $T=0.07$  hours and for  $T=0.27$  hours. The calculations were carried out with a step of 0.005 hours, half of the radius of the star being fixed. It is evident that the most stable part is the vicinity of  $R_0$ . For  $r > 3R_{3B}/4$  the increase of velocity is less significant.

/63

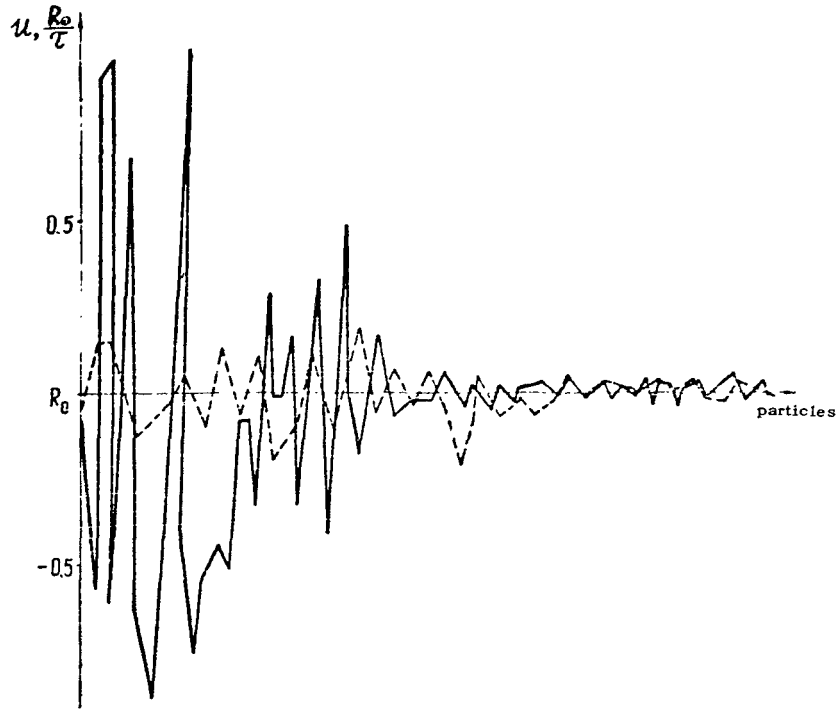


Figure 4. The Dependency  $u(r)$  at Time  $T = 213 \Delta t$ ;  $R_0 = R_{03} B^{1/4}$ ;  $\Delta t = 0.0005$  Hours; - - -  $h = R_{03} B^{200}$ ; —  $h = R_{03} B^{400}$ .

Let us introduce the following distribution of velocity:  $u = 6R_{\odot} / \tau$  for  $0 \leq r \leq R_0$ ,  $u = 0$  for  $r > R_0$ . This is equivalent to the formation of a shock wave. Calculations were performed with  $R_0 = R_{03} B^{1/3}$  ( $\tau = 1$  hour;  $R_{\odot}$  is the radius of the sun);  $t = 0.0001$  hours.

The initial  $P$ ,  $\rho$ ,  $T$  were taken from the results of the calculation of the uniform model. The calculations showed that the shock wave front diffuses with the course of time (Fig. 8), which indicates the existence of viscosity, not taken into account by the usual PIC method.

One of the defects of the method consists in the crossover of particles. This phenomenon can be averted in the following way. Let  $v$ ,  $r$  be the velocity and the coordinate of a particle;  $v$  is interpolated relative to the cells

$$v = u_i + \frac{u_{i+1} - u_i}{r_{i+1} - r_i} (r - r_i). \quad (8)$$



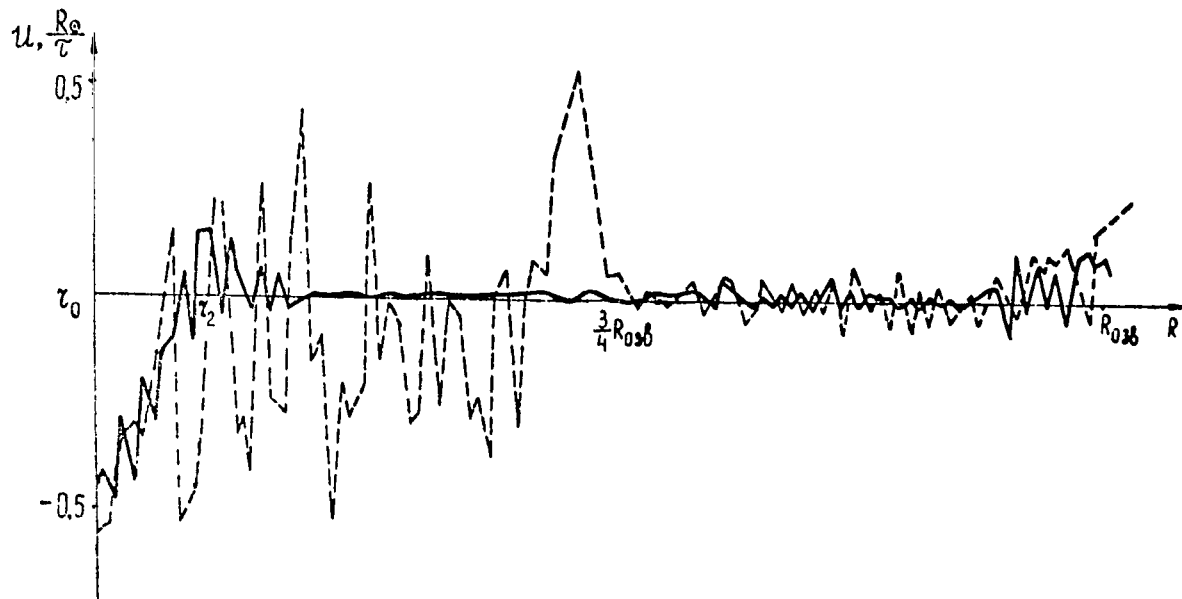


Figure 5. The Dependency  $u(r)$  at Times  $T_1 = 14\Delta t$ ;  $T_2 = 54\Delta t$ ;  $\Delta t = 0.005$  Hours;  
 $R_0 = R_{03B}/2$ ; ———  $14\Delta t$ ; - - - - -  $54\Delta t$ .

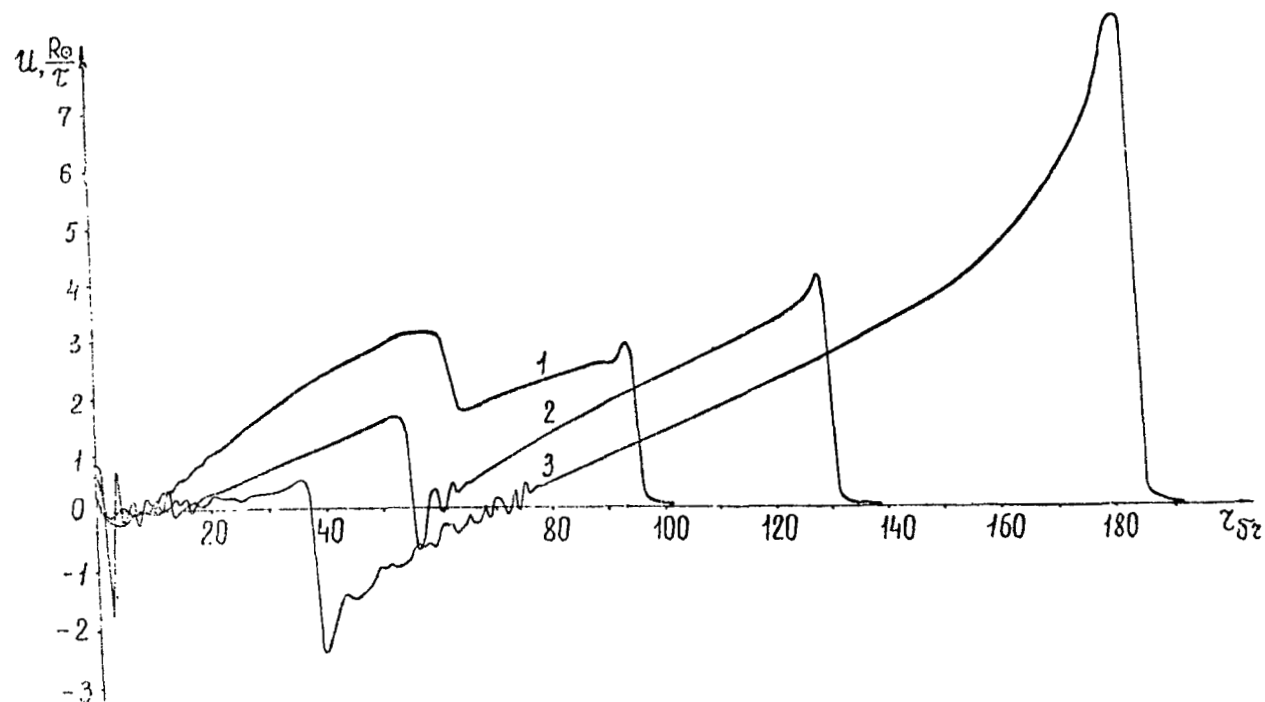


Figure 6a. The Dependency  $u(r)$  at Times  $T_1 = 0.768$  Hours;  $T_2 = 0.1536$  Hours;  $T_3 = 0.2304$  Hours;  $u = 6R_0 / \tau$  for  $r \leq R_0$ ;  $u = 0$  for  $r > R_0$ ;  $R_0 = R_{03}B^{1/3}$ .

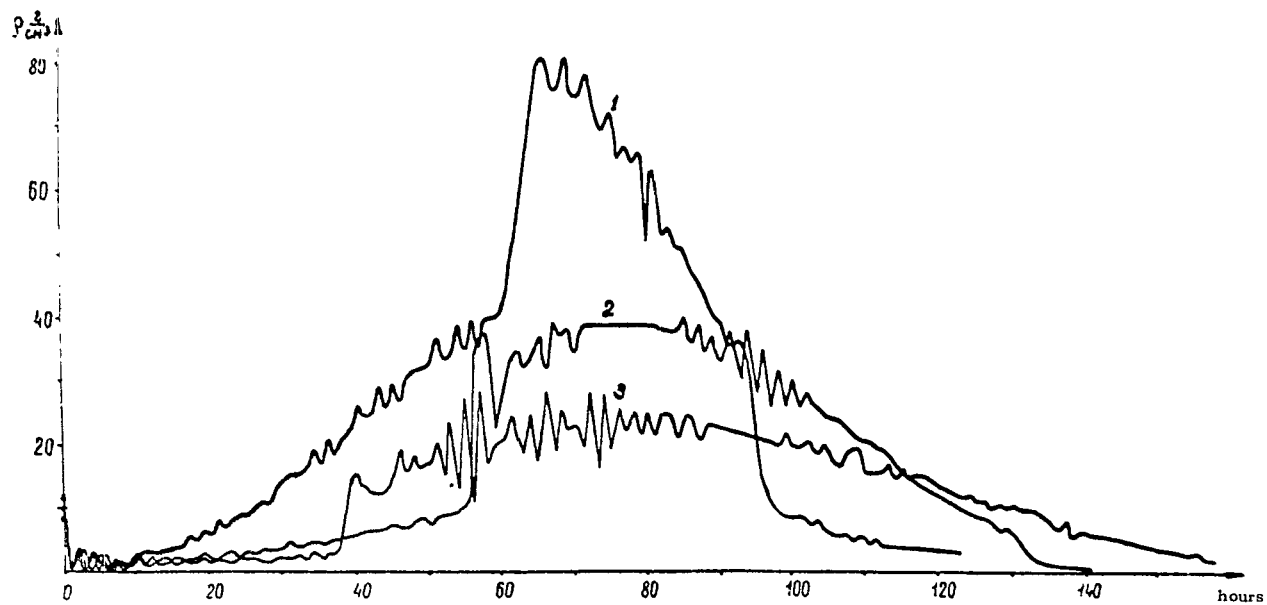


Figure 6b. The Dependency  $\rho(r)$  at Times  $T_1 = 0.0768$  Hours;  $T_2 = 0.1536$  Hours;  $T_3 = 0.2304$  Hours;  $u = 6R_{\odot} / \tau$  for  $r \leq R_0$ ;  $u = 0$  for  $r > R_0 \cdot R_{03B}^{1/3}$ .

In the interval  $\Delta t$  the velocities of the cells do not change. At time  $t_m$ ,  $r = r_0$ . Solution of (8) gives

$$r(t) = e^{\frac{(u_{i+1} - u_i) \Delta t}{r_{i+1} - r_i}} \left\{ r_0 + \frac{(u_{i+1} r_i - u_i r_{i+1})}{u_{i+1} - u_i} \left( e^{-\frac{u_{i+1} - u_i}{r_{i+1} - r_i}} - 1 \right) \right\}$$

$$\Delta t = t - t_m.$$

If a particle crosses the middle of the  $i$ -th cell at time  $t' = t_m + \Delta t'$ , and falls into interval 2 (see Fig. 2), then

$$r(t) = e^{\frac{(u_i - u_{i-1})(t - t')}{r_i - r_{i-1}}} \left\{ r_0' + \frac{(u_i r_{i-1} - u_{i-1} r_i)}{u_i - u_{i-1}} \left( e^{-\frac{u_i - u_{i-1}}{r_i - r_{i-1}}} - 1 \right) \right\}$$

$$r_0' = e^{\frac{(u_{i+1} - u_i) \Delta t'}{r_{i+1} - r_i}} \left\{ r_0 + \frac{(u_{i+1} r_i - u_i r_{i+1})}{u_{i+1} - u_i} \left( e^{-\frac{u_{i+1} - u_i}{r_{i+1} - r_i}} - 1 \right) \right\}.$$

Particles in the interval  $\Delta t$  do not cross over. One must turn attention to artificial viscosity in equations (7) and to a rational distribution of particles and cells (for example, a combination of a and b). The instabilities portrayed in Fig. 4 can be significantly decreased.

In conclusion it should be noted that, despite the limited possibilities of the method of "particles in cells" for the calculation of the evolutions of stars, as it appears to us, this methodology is applicable to the analysis of explosive processes.

## REFERENCES

1. Schwartzschild, M. Structure and Evolution of Stars. Publishing House of Foreign Literature, Moscow, 1961.
2. Henyey, L.G., K.H. Bohm, R. Levier, and R.D. Levee. Astrophys. J., 1959, 129, No. 3.

3. Lomnev, S. P. The Effect of Coulomb Repulsion on Particle Bunching in A Linear Election Accelerator. Dokl. Akad. Nauk SSSR, 1960, 135, 4.
4. Harlow, F. H., D. O. Dickman, D. E. Harris, and R. E. Martin, Two-Dimensional Hydrodynamic Calculations. Los Alamos Scientific Laboratory Report, 1959, No. La-2301.

Translated for the National Aeronautics and Space Administration by  
Scripta Technica, Inc. NASW-2036.

NATIONAL AERONAUTICS AND SPACE ADMINISTRATION

WASHINGTON, D. C. 20546

OFFICIAL BUSINESS

PENALTY FOR PRIVATE USE \$300

FIRST CLASS MAIL



POSTAGE AND FEES PAID  
NATIONAL AERONAUTICS AND  
SPACE ADMINISTRATION

019 001 C1 U 19 710716 S00903DS  
DEPT OF THE AIR FORCE  
WEAPONS LABORATORY /WL0L/  
ATTN: E LOU BOWMAN, CHIEF TECH LIBRARY  
KIRTLAND AFB NM 87117

POSTMASTER: If Undeliverable (Section 158  
Postal Manual) Do Not Return

*"The aeronautical and space activities of the United States shall be conducted so as to contribute . . . to the expansion of human knowledge of phenomena in the atmosphere and space. The Administration shall provide for the widest practicable and appropriate dissemination of information concerning its activities and the results thereof."*

— NATIONAL AERONAUTICS AND SPACE ACT OF 1958

## NASA SCIENTIFIC AND TECHNICAL PUBLICATIONS

**TECHNICAL REPORTS:** Scientific and technical information considered important, complete, and a lasting contribution to existing knowledge.

**TECHNICAL NOTES:** Information less broad in scope but nevertheless of importance as a contribution to existing knowledge.

**TECHNICAL MEMORANDUMS:**  
Information receiving limited distribution because of preliminary data, security classification, or other reasons.

**CONTRACTOR REPORTS:** Scientific and technical information generated under a NASA contract or grant and considered an important contribution to existing knowledge.

**TECHNICAL TRANSLATIONS:** Information published in a foreign language considered to merit NASA distribution in English.

**SPECIAL PUBLICATIONS:** Information derived from or of value to NASA activities. Publications include conference proceedings, monographs, data compilations, handbooks, sourcebooks, and special bibliographies.

**TECHNOLOGY UTILIZATION PUBLICATIONS:** Information on technology used by NASA that may be of particular interest in commercial and other non-aerospace applications. Publications include Tech Briefs, Technology Utilization Reports and Technology Surveys.

*Details on the availability of these publications may be obtained from:*

**SCIENTIFIC AND TECHNICAL INFORMATION OFFICE**

**NATIONAL AERONAUTICS AND SPACE ADMINISTRATION**

**Washington, D.C. 20546**